

STARS


University of Central Florida
STARS

Electronic Theses and Dissertations, 2004-2019

2004

Performance Analysis Of Low-power, Short-range Wireless Transceivers

Usha Neupane
University of Central Florida

 Part of the [Electrical and Electronics Commons](#)
Find similar works at: <https://stars.library.ucf.edu/etd>
University of Central Florida Libraries <http://library.ucf.edu>

This Masters Thesis (Open Access) is brought to you for free and open access by STARS. It has been accepted for inclusion in Electronic Theses and Dissertations, 2004-2019 by an authorized administrator of STARS. For more information, please contact STARS@ucf.edu.

STARS Citation

Neupane, Usha, "Performance Analysis Of Low-power, Short-range Wireless Transceivers" (2004).
Electronic Theses and Dissertations, 2004-2019. 217.
<https://stars.library.ucf.edu/etd/217>



PERFORMANCE ANALYSIS OF LOW-POWER, SHORT-RANGE WIRELESS
TRANSCEIVERS

by

USHA NEUPANE
B.E. Regional Engineering College, 2001

A thesis submitted in partial fulfillment of the requirements
for the degree of Master of Science
in the Department of Electrical and Computer Engineering
in the College of Electrical and Computer Engineering
at the University of Central Florida
Orlando, Florida

Fall Term
2004

Major Professor: Dr. Samuel M. Richie

© 2004 Usha Neupane

ABSTRACT

To address the various emerging standards like Bluetooth™, Home RF, Wi-fi™ (IEEE 802.11), ZigBee™ etc., in the field of wireless communications, different transceivers have been designed to operate at various frequencies such as 450 MHz, 902-920 MHz, 2.4 GHz, all part of designated ISM band. Though, the wireless systems have become more reliable, compact and easy to develop than before, a detailed performance analysis and characterization of the devices should be done.

This report details the performance analysis and characterization of a popular binary FSK transceiver TRF6901 from Texas Instruments. The performance analysis of the device is done with respect to the TRF/MSP430 demonstration and development kit.

ACKNOWLEDGMENTS

I would like to express my gratitude to my advisor Dr. Samuel Richie, for his constant support, guidance and valuable advice for the completion of this work and my graduate studies.

I am very grateful to Dr. Parveen Wahid and Dr. Bernard C. Deloach Jr for their valuable ideas and expertise and help in the antenna measurements. I would also like to thank Dr. Malocha for the practical RF design skills he taught in the RF and microwave communication class.

I would like to thank my colleagues, especially, Tommy, Tripti and Anand for their enormous help and support in the completion of my work.

TABLE OF CONTENTS

LIST OF FIGURES	ix
LIST OF TABLES	xi
1 INTRODUCTION.....	1
1.2 Structure of Wireless Transceivers	3
1.3 Performance Criteria of Wireless Transceivers	5
1.4 Thesis Overview	6
2 WIRELESS TRANSCEIVERS.....	7
2.1 TRF6901 Transmitter Architecture.....	7
2.1.1 Integer N-Synthesizer	8
2.1.1.1 VCO	10
2.1.1.2 Main and Reference Divider	11
2.1.1.3 Phase detector and charge pumps	11
2.1.1.4 Loop Filter	12
2.1.1.5 Loop Filter and VCO Equations	13
2.1.2 Power Amplifier.....	13
2.1.3 DC-DC Converter	14
2.1.4 Brownout Detector.....	14
2.2 TRF6901 Receiver Architecture.....	14
2.2.1 LNA	16

2.2.2 Mixer.....	16
2.2.3 IF Amplifier and Limiter	16
2.2.4 Received Signal Strength Indicator	17
2.2.5 Demodulator	17
2.2.6 Low-pass Filter and Post-detection Amplifier	18
2.2.7 Data Slicer.....	19
2.3 Serial Interface	20
2.3.1 Clock Output Buffer	20
2.4 Designing an application with TRF6901	20
2.4.1 Data Rate.....	21
2.4.2 Data Coding	21
2.4.3 FSK Modulation Theory	24
2.5 Studied Module TRF6901/MSP430 Demonstration and Development Kit	25
2.5.1 Hardware Overview	26
2.5.1.1 MSP430F449	27
2.5.1.2 Embedded Antenna.....	28
3 RANGE ESTIMATION.....	30
3.1 Factors determining range.....	30
3.1.1 Line-of-sight	31
3.1.2 Transmitter and Receiver Line Losses.....	32
3.1.3 Power Output and Receiver Sensitivity	32
3.1.4 Transmit and Receive Antenna Gain	33

3.1.4.1 Absolute Gain Measurements	34
3.1.4.2 Gain - Transfer Measurements.....	35
3.1.5 Path loss	35
3.2 Experiments on Range	37
3.2.1 Antenna measurements	37
3.2.1.1 Determination of the antenna pattern of the on-board PCB antenna	37
3.2.1.1.1 Instruments Used	38
3.2.1.1.2 Testing Method	39
3.2.1.1.3 Experimental Results	42
3.2.1.1.3.1 Experiment 1	42
3.2.1.1.3.2 Experiment 2	44
3.2.1.1.3.3 Experiment 3	46
3.2.1.1.3.4 Experiment 4	48
3.2.1.1.3.5 Experiment 5	50
3.2.1.2 Determination of the gain of TX and RX on-board PCB antenna	52
3.2.1.3 Pattern Measurement with external dipole	55
3.2.2 Power Measurements	60
3.2.2.1 Transmitted Power	60
3.2.2.2 Receiver Sensitivity	60
3.2.3 Path loss	61
3.2.4 Link Distance Calculation.....	61
3.3 Simulation Results	62

3.4 Suitable Candidate Antennas for Short-Range Radio Applications	65
4 CONCLUSION	67
LIST OF REFERENCES	68

LIST OF FIGURES

Figure 1: Transmitter Block Diagram.....	4
Figure 2: Receiver Block Diagram	4
Figure 3: TRF6901 Transmitter block diagram [3]	8
Figure 4: TRF6901 PLL and Clock Circuit.....	10
Figure 5: External Loop Filter	12
Figure 6: TRF6901 receiver block diagram [3]	15
Figure 7: FM Demodulator Block Diagram.....	17
Figure 8: External discrete component tank circuit	18
Figure 9: Post-Detection Amplifier/Low-Pass Filter	19
Figure 10: Data Slicer	19
Figure 11: Common digital base band encoding schemes.....	22
Figure 12: Binary FSK signal generation	25
Figure 13: TRF6901/MSP430 Demonstration and Development kit	26
Figure 14: MSP430x44x functional block diagram.....	27
Figure 15: MSP-TRF6901 Demo kit	29
Figure 16: Free space path loss as a function of distance @ 915 MHz	36
Figure 17: Experimental Setup of on board PCB antenna of TRF6901 Demonstration and Development kit configured in transmitting mode and a yagi antenna in receiving mode.	40
Figure 18: Short bursts of data pulses received by the MA shown in Wiltron 560A Network Analyzer.....	41

Figure 19: Experimental Setup	42
Figure 20: Horizontal Polarization of the embedded antenna	43
Figure 21: Experimental Setup	45
Figure 22: Vertical Polarization of the embedded antenna.....	45
Figure 23: Experimental Set up	47
Figure 24: Cross-polarization pattern	47
Figure 25: Experimental Set up	49
Figure 26: Cross-polarization pattern	49
Figure 27: Experimental Set up	51
Figure 28: Cross-polarization pattern	51
Figure 29(a) Experimental Set up for the gain measurement of the Yagi antenna.....	53
Figure 30: Experimental Setup for determining the gain of the embedded antenna	55
Figure 31: Experimental Setup	56
Figure 32: Measured pattern data of external dipole antenna.....	56
Figure 33: Experimental Setup	58
Figure 34: Measured pattern data of external dipole antenna connected to TRF/MSP430 board	58
Figure 35: Experimental Setup for the receiver sensitivity measurement	60
Figure 36: Structure of the simulated antenna	63
Figure 37: Return loss of the onboard PCB antenna from simulation.....	64
Figure 38: Simulated pattern of the on-board PCB antenna	65

LIST OF TABLES

Table 1: Short-range radio applications	2
Table 2: PCM Binary Coding Methods	23
Table 3: Instruments Used	38
Table 4: Horizontal Polarization data referred to experiment 1	44
Table 5: Vertical Polarization data referred to experiment 2.....	46
Table 6: Cross-polarization data referred to experiment 3	48
Table 7: Cross-polarization data referred to experiment 4	50
Table 8: Cross-polarization data referred to experiment 5	52
Table 9: External dipole horizontal polarization data without connecting to TRF6901 board	57
Table 10: External dipole horizontal polarization data with connecting to TRF6901 board.....	59
Table 11: Link Calculation Results.....	62

1 INTRODUCTION

1.1 Short-range Wireless Applications

Dating back to the 1970s, there were a limited number of short-range radio applications in use. The applications suffered significant drawbacks such as frequency drift and susceptibility to interference [1]. But in the recent years, there has been a wide-spread use of wireless applications. This is due to the technological developments such as semiconductor reduction, single-chip mixed signal ICs, more efficient digital modulation techniques, better solid-state devices and efficient and compact antennas. Various standards such as Bluetooth TM, Home RF, Wifi (IEEE 802.11) and ZigBee have emerged rapidly in recent years.

Short-range wireless applications are those applications usually operated in the unlicensed ISM (industrial scientific medical) band with RF power output of several microwatts up to 100 milliwatts with a resulting communication range of several centimeters up to several hundred meters. The applications are usually designed for indoor operation with omnidirectional, built-in antennas with battery operated transmitters or receivers. The major difference between the short range devices and the Bluetooth/802.11 devices is the implementation of advanced and complicated protocol stacks in the hardware. Usually, for the short-range devices the protocol stacks are simple despite some limitations. Table 1.1 lists some short-range radio applications and their characteristics. [1]

Table 1: Short-range radio applications

Application	Frequencies	Characteristics
Security Systems	300-500 MHz, 800 MHz, 900 MHz	Simplicity, easy installation
Emergency Medical Alarms	300-500 MHz, 800 MHz	Convenient carrying, long battery life, reliable
Computer Accessories- mouse, keyboard	328.6 MHz – 2.9 GHz	High data rates, very short range, low cost
RFID (Radio Frequency Identification)	100 KHz - 2.4 GHz	Very short range, active or passive transponder
WLAN (Wireless Local Area Network)	900 MHz, 2.4 GHz	High continuous data rates, spread-spectrum modulation, high price
Wireless microphones, Wireless Headphones	30 MHz- 328.6 MHz, 328.6 MHz – 2.9 GHz	Analog high-fidelity voice modulation, moderate price
Keyless Entry- Gate openers	328.6 MHz – 2.9 GHz	Miniature transmitter, special coding to prevent duplication
Wireless bar code readers	900 MHz, 2.4 GHz	Industrial use, spread spectrum, expensive

To address the mentioned applications, various transmitters, receiver and transceiver integrated circuits (ICs) are available from different manufacturers. The ICs are designed for different frequency bands employing different modulation schemes and for different emerging standards. The transceiver ICs such as MICRF501, MAX2420 series, TRF6900 series, CC2400 etc. are common available ones in the market for the popular ISM band. The low price and small size makes them popular among consumers.

1.2 Structure of Wireless Transceivers

A typical wireless transceiver consists of a transmitter and receiver subsection embedded on a single chip. A transmitter generally is comprised of a VCO (Voltage Controlled Oscillator), PLL (Phase Locked Loop), power amplifier and a modulator of some specific technique while the receiver is comprised of the LNA (Low Noise Amplifier), mixer, filter, demodulator, a comparator and slicer. Within most transceiver architectures, the PLL and VCO are shared between transmit and receive modes thereby operating in half-duplex modes, but may be duplicated if full-duplex is needed.

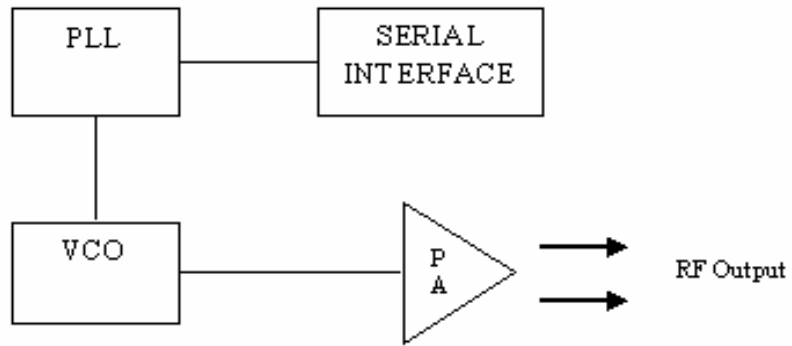


Figure 1: Transmitter Block Diagram

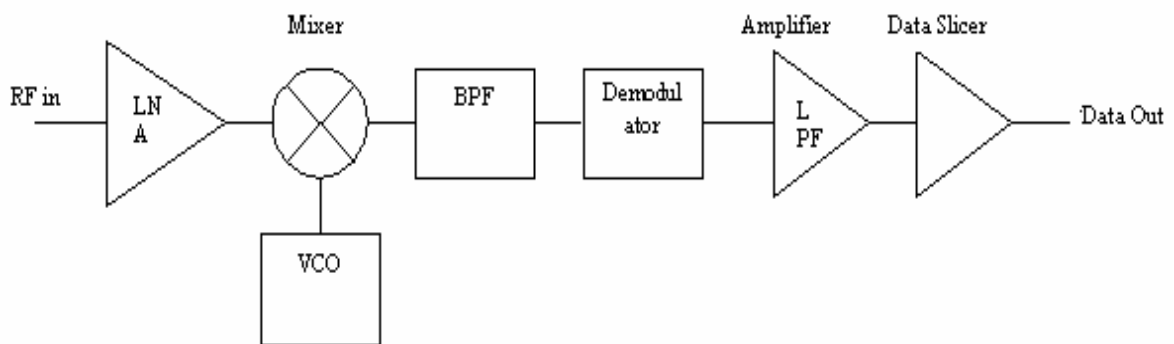


Figure 2: Receiver Block Diagram

1.3 Performance Criteria of Wireless Transceivers

An important parameter for rating a wireless system is its practical range. A RF (radio frequency) link differs from a wired one with respect to some critical facts. Radio frequencies being a shared medium occupy the same propagation medium with many competing signals which makes it more prone to interference. Therefore, the inherent reliability of a RF link is lower than the wired link. Moreover, wireless connections are diverse: they differ in frequency spectrum, range, bandwidth, modulation scheme, interference sources and physical environment. There are certain regulations governing the use of RF spectrum to avoid the interference. Generally, a license is required to operate a radio transmitter. In the U.S (United States), the FCC (Federal Communications Commission) regulates the radio usage. The 27 MHz, 260 MHz to 470 MHz, 902 MHz to 928 MHz and the 2.4 GHz bands are the most commonly used bands allocated for general use. The 260 MHz to 470 MHz band has restrictions on the types of data to transmit while 902 MHz -928 MHz and the 2.4 GHz is the most commonly used unrestricted band.

The range of a device depends heavily on the conditions of the measurement. The characteristics of the transmitting and receiving antennas, orientation, height above ground and the application circuitry affect range. Usually, manufacturers do not document the characteristics of their devices based on the operating conditions. The user has to perform a detailed analysis on the performance of the device. The focus of this thesis work is a detailed performance analysis

and characterization of the new generation wireless transceivers, with special emphasis on TRF6901, a popular binary FSK device from TI (Texas Instruments, Inc).

The TRF6901 is a single chip RF transceiver designed for the 868-MHz and 915-MHz ISM band operating at 1.8-V to 3.6-V with low power consumption, and giving 9-dBm typical output power. It is intended for use as a low cost FSK or OOK transceiver to establish a frequency-programmable, half-duplex, bidirectional RF link.

1.4 Thesis Overview

This thesis details the performance analysis and characterization of short-range wireless transceivers with special emphasis on the TI TRF6901. Since a very important factor in the characterization of a wireless device is its range, different experiments such as antenna measurements, power measurements, and losses determination were carried out. The report is organized in four chapters. Chapter 2 describes the architecture of the TRF6901 and one of the applications designed by TI. Chapter 3 discusses the range determination overview, factors affecting range performance and the detailed experimental results. Finally, Chapter 4 is the conclusion.

2 WIRELESS TRANSCEIVERS

This chapter outlines the basic elements of a RF transceiver with special emphasis on the TRF6901, a low-cost transceiver produced by Texas Instruments. The better noise and distortion immunity, viability of regenerative repeaters, flexible hardware implementation, efficient coding and multiplexing schemes and of course, the relentless exponential progress in digital technology has made digital communication more popular, superior and reliable over analog communication [2]. The increase in demand for data transmission during the last four to five decades resulted in the development of more sophisticated ICs supporting digital communication. TRF6901 falls under one of these new generation ICs intended to be used for digital FSK and OOK modulated applications.

2.1 TRF6901 Transmitter Architecture

The transmitter consists of an integrated VCO (voltage controlled oscillator) and a tank circuit, a complete integer-N synthesizer, and a PA (power amplifier). The divider, prescaler and reference oscillator require only the addition of an external crystal and a loop filter to provide a complete PLL (phase locked loop) with a typical frequency resolution of better than 200 KHz [3][4]. These are shown in figure 3.

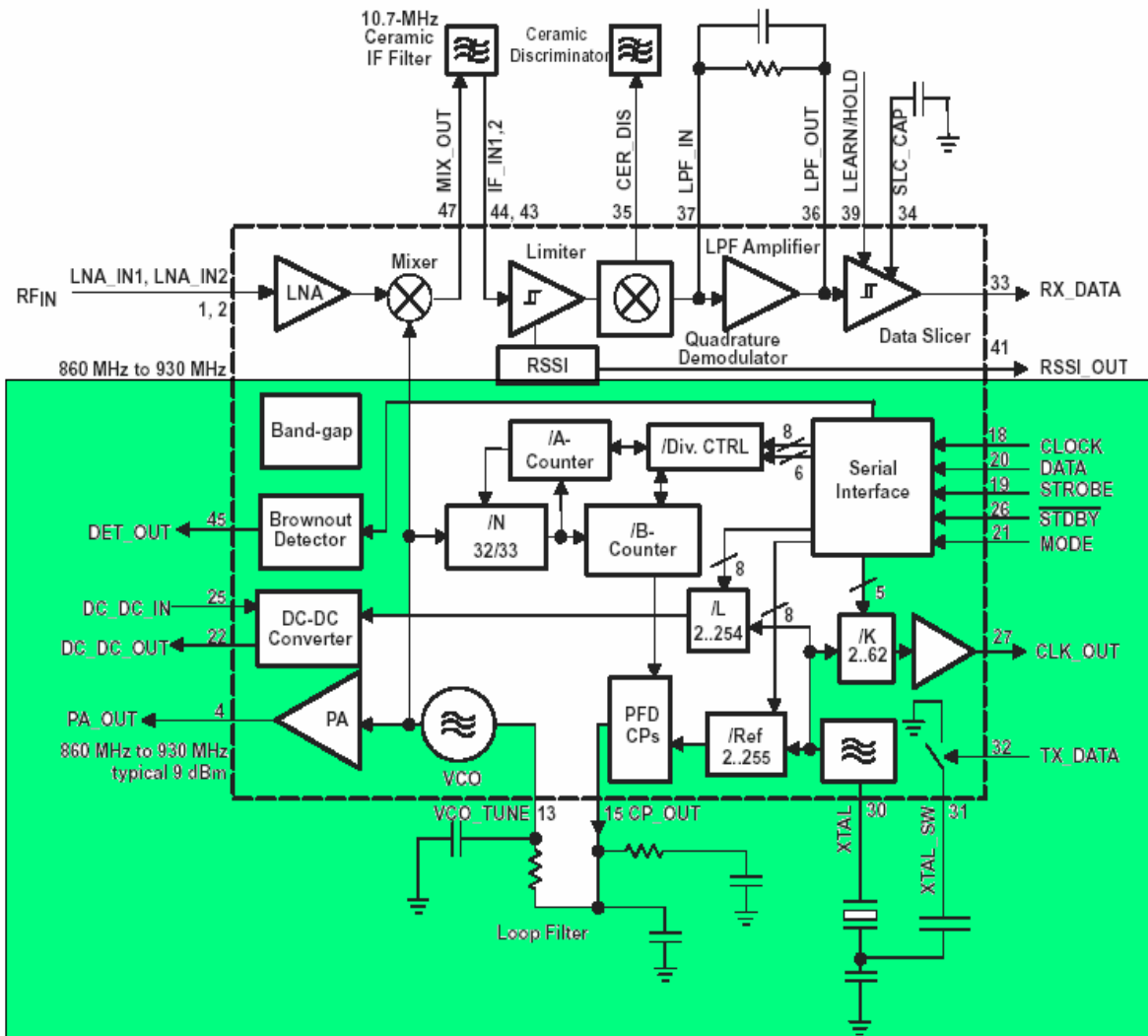


Figure 3: TRF6901 Transmitter block diagram [3]

2.1.1 Integer N -Synthesizer

The integer N -PLL is the radio frequency synthesizer for the TRF6901. It is used to generate the transmit signal. It also functions as the local oscillator for the receive mixer. A PLL circuit consists of four basic components namely, VCO, PFD (phase frequency detector), main

and reference divider and loop filter. The PLL circuit performs frequency multiplication via a negative feedback to generate output frequency F_{VCO} in terms of phase detector comparison frequency F_R [5]. The signal (F_X) from a reference crystal oscillator is divided by an integer factor R down to F_R which is used by the phase detector to tune the VCO.

$$F_{PD} = F_{VCO} \div N, \text{ where } F_{VCO} = F_{OUT}$$

$$F_R = F_X \div R, \text{ where } 1 \leq R \leq 256$$

The minimum frequency resolution and thus the minimum channel spacing is F_R .

$$\text{With } F_R = F_{PD} \text{ under locked conditions, } F_{OUT} = \frac{F_X N}{R} = (A + 32B)F_R$$

When the PLL is in unlocked state, the phase detector compares the divided VCO signal to the divided crystal frequency and implements an error signal from two charge pumps. The error signal corrects the VCO output to the desired frequency. The PLL and clock diagram is shown in figure 4.

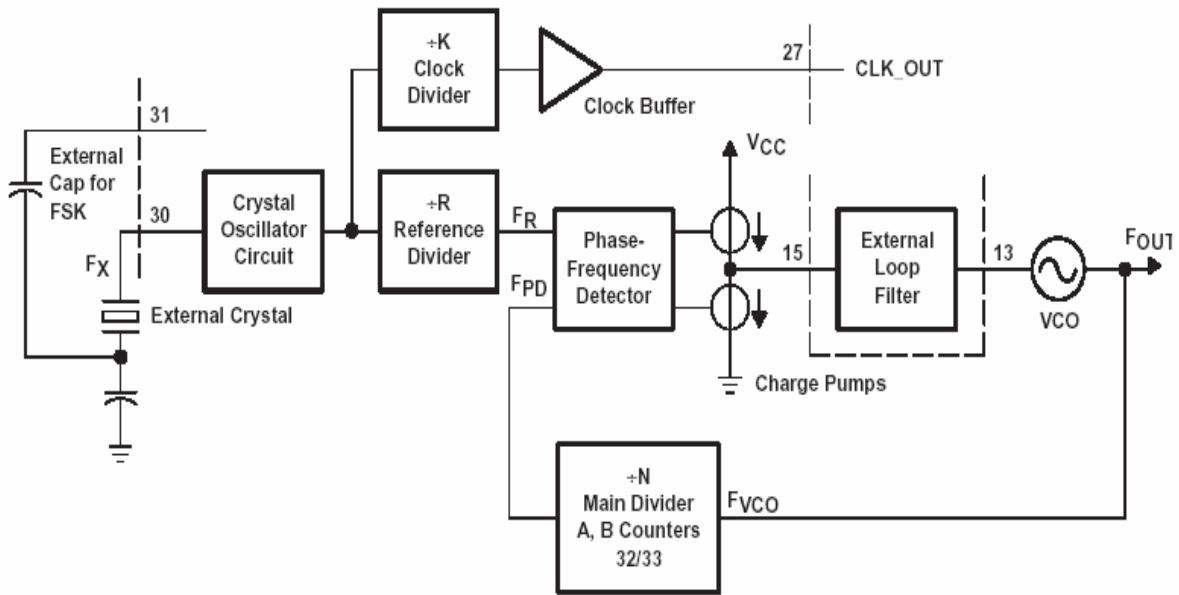


Figure 4: TRF6901 PLL and Clock Circuit

2.1.1.1 VCO

The VCO produces an RF output signal with a frequency that is dependent upon the DC-tuning voltage at terminal 13. VCOs are positive feedback amplifiers with a tuned resonator tank circuit in the feedback loop. The tank circuit is passive and has integrated varactor diodes and inductors. TRF6901 has an integrated VCO and tank circuit. The VCO has an open-loop operating band from approximately 700 MHz to 1 GHz with open loop gain approximately 110 MHz/V [3].

2.1.1.2 Main and Reference Divider

The main divider is a 5-bit A counter, a 9-bit B counter and a prescaler. The total divide by N operation is related to the 32/33 prescaler by,

$$N_{\text{TOTAL}} = 33 \times A + 32 \times (B - A),$$

where $0 \leq A \leq 31$ and $31 \leq B \leq 551$

The reference divider reduces the frequency of the external crystal (F_X) by an 8-bit programmable integer divisor to an internal reference frequency (F_R) used for the phase-locked loop. The internal reference frequency determines the lock time, maximum data rate, noise floor and loop filter design.

2.1.1.3 Phase detector and charge pumps

The phase detector generates the error signal required in the feedback loop of the synthesizer. The phase detector is the phase frequency design as it resolves phase difference in $\pm 2\pi$ range or more. It operates in three modes namely,

- Frequency detect in which the output of the charge pump will be a constant current integrated by the loop filter to produce a continuously changing voltage applied to the VCO.

- Phase detect in which the charge pump will be active only for a portion of each phase detector cycle and is proportional to the phase difference between the two signals.
- Phase locked in which the phase difference between the two signal reaches zero.

The gain is given by,

$$K_p = \frac{I_{(CP)}}{2\pi}$$

, where $I_{(CP)}$ is the peak charge pump current.

2.1.1.4 Loop Filter

The loop filter is typically a second or third-order passive design. The bandwidth of the filter should be wide in-order to relock the PLL as the FSK frequency is toggled when sending data. The loop filter should also be wider than the data modulation rate. Figure 5 shows a typical third order passive filter circuit.

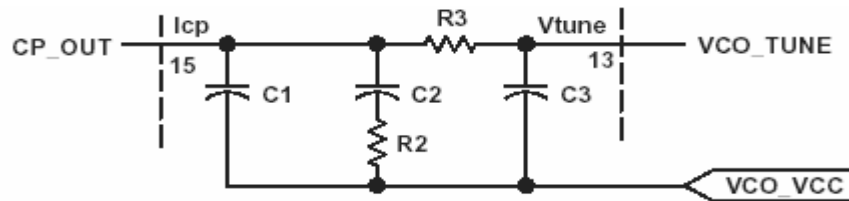


Figure 5: External Loop Filter

2.1.1.5 Loop Filter and VCO Equations

The loop filter and VCO are defined by the following parameters.

B_L = bandwidth of loop filter

f_R = PLL reference frequency, Hz

f_M = modulation rate, symbol rate, or maximum rate at which FSK frequencies are toggled, Hz

K_p = phase-frequency detector

I_{CP} = charge pump current, mA

K_{VCO} = VCO gain, design value is approximately 110 MHz/V

$$B_L \approx 1.2 \times f_M$$

$$B_L \approx \frac{f_R}{5}$$

$$K_p = \frac{I_{CP}}{2\pi}$$

$$f_R \approx 6 \times f_M$$

2.1.2 Power Amplifier

The power amplifier has four programmable states: full power, 10-dB attenuation, 20-dB attenuation and off [3]. During the receive mode, the PA is powered down with the VCO still

operating. During FSK or OOK operation, the TX_DATA signal turns the PA on and off according to the data incident on that pin.

2.1.3 DC-DC Converter

The main purpose of the DC-DC converter is to provide an adequate voltage to the charge pumps and VCO core if the supply voltage drops down to 1.8 V. The switching frequency is adjustable through a clock divider that reduces the external clock frequency by a C-word programmable factor (L) of 2 to 254 in steps of 2. The DC-DC converter is designed to operate at a switching frequency of around 1 MHz [3].

2.1.4 Brownout Detector

The brownout detector provides an output voltage to indicate a low supply voltage. The threshold is set with the B word [3]. Four different thresholds are available. During operation, the brownout detector is always enabled and during stand-by, it is disabled.

2.2 TRF6901 Receiver Architecture

The integrated receiver of TRF6901 can be used as a single-conversion FSK/OOK receiver. It consists of a LNA (low noise amplifier), mixer, limiter, FM/FSK demodulator with

an external tank LC tank circuit or ceramic discriminator, RSSI (received signal strength indicator), a LPF (low pass filter), post detection amplifier and a data slicer. These are shown in figure 6.

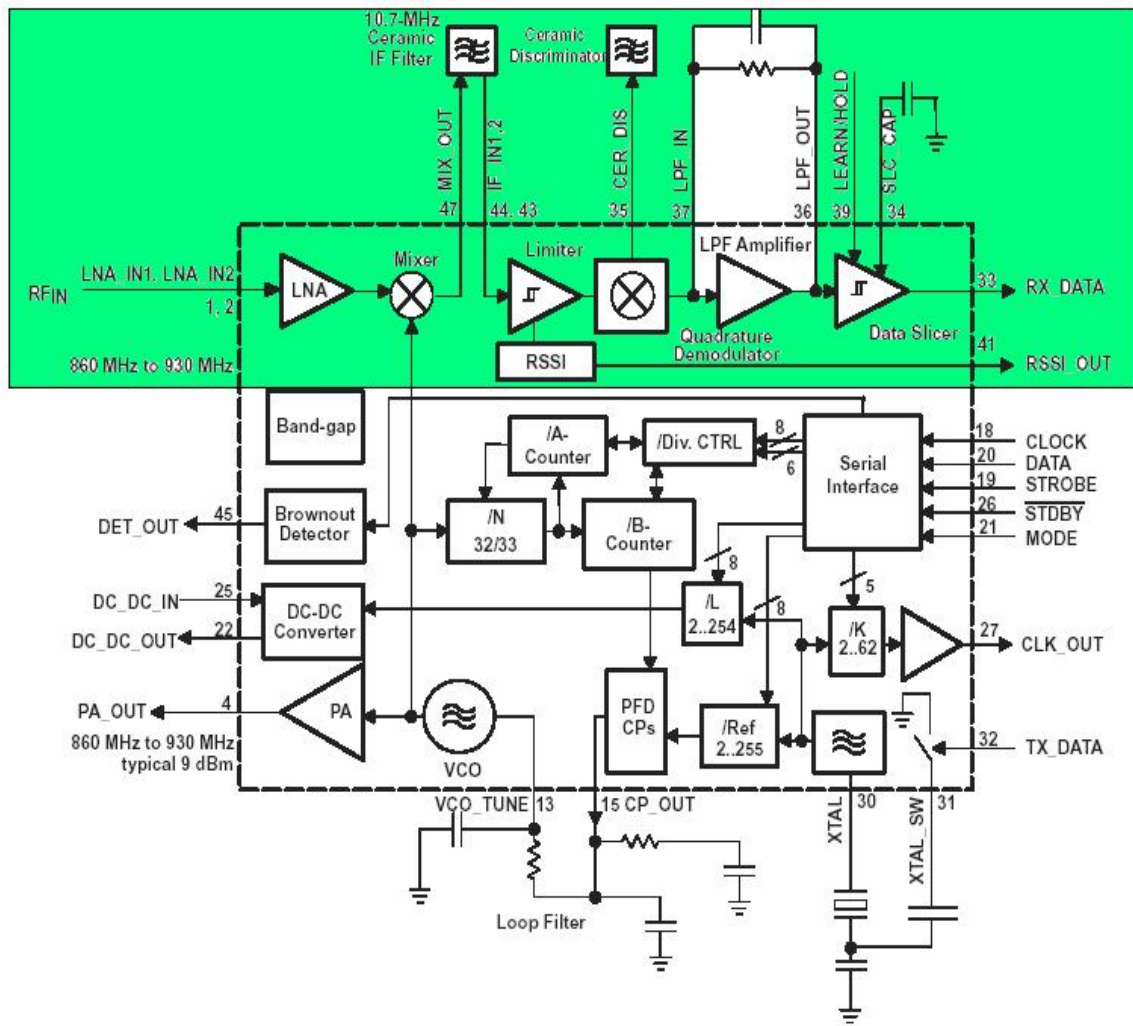


Figure 6: TRF6901 receiver block diagram [3]

2.2.1 LNA

The LNA has differential inputs with an impedance of approximately $500\ \Omega$ in parallel with $0.7\ \text{pF}$ [3]. The off-chip input matching network has the dual task of matching a $50\ \Omega$ connector to the differential inputs and providing a 180 degree phase shift between the inputs at terminals 1 and 2. The predicted noise figure of the LNA and the input matching network is $2.5\ \text{dB}$ [3].

2.2.2 Mixer

The mixer operates with the on-chip VCO and generates a signal at the IF (intermediate frequency) of $10.7\ \text{MHz}$. The mixer offers good linearity (high IP3). An external matching network is required to transform the output impedance of the mixer ($1.4\ \text{K}\Omega$) to the input impedance of the IF filter (330Ω) [3].

2.2.3 IF Amplifier and Limiter

The IF amplifier amplifies the output waveform from the mixer. It has differential inputs to its first stage. It provides $86\ \text{dB}$ of gain and input impedance of $330\ \Omega$ [3].

The limiting amplifier removes the amplitude variations from the IF waveform. It provides $68\ \text{dB}$ of gain [3].

2.2.4 Received Signal Strength Indicator

The RSSI (received signal strength indicator) voltage is proportional to the log of the down-converted RF signal at the IF limiting amplifier input. It is a temperature compensated circuit and is useful for detecting interfering signals, transceiver handshaking and RF channel selection. It has a slope of 20mV/dB [3].

2.2.5 Demodulator

The quadrature demodulator decodes digital frequency shift keying (FSK) modulation. It is optimized for use with a ceramic discriminator. A quadrature-demodulator circuit is used as shown in Figure 7 [6].

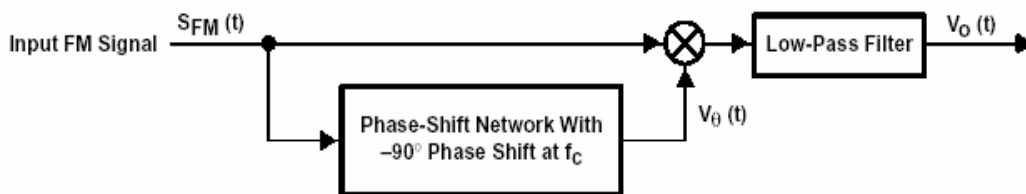


Figure 7: FM Demodulator Block Diagram

The phase shift network can be either an external RLC tank circuit or ceramic discriminator. Figure 8 shows an external RLC tank circuit. The resonant frequency of the

external RLC discriminator can be calculated from the inductor and capacitor values used in the circuit.

$$f_{\text{res}} = \frac{1}{2\pi\sqrt{LC}}$$

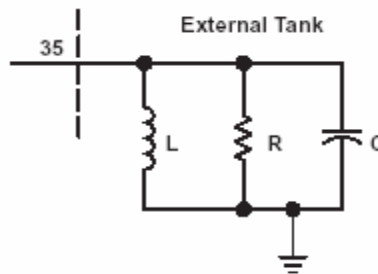


Figure 8: External discrete component tank circuit

2.2.6 Low-pass Filter and Post-detection Amplifier

The low-pass filter and the post detection amplifier amplify the output of the demodulator circuit and provide filtering of unwanted products from the demodulator circuit. The post-detection amplifier operates as a low-pass trans-impedance amplifier. The external low-pass filter circuit must be optimized for the data rate. The 3-dB corner frequency of the low-pass filter should be greater than twice the data rate.

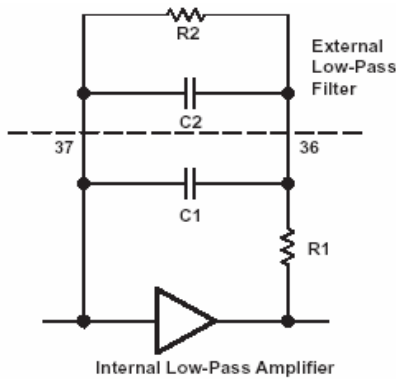


Figure 9: Post-Detection Amplifier/Low-Pass Filter

2.2.7 Data Slicer

The data slicer is a comparator circuit for received digital (FSK) data. The data slicer output voltage depends on the difference between the received signal and a reference voltage used as a decision threshold. The external S&H (sample and hold) capacitor is charged up to the average dc voltage in the learn mode to establish a reference voltage before a sequence of actual data is received in the hold mode. The data slicer is shown in figure 10.

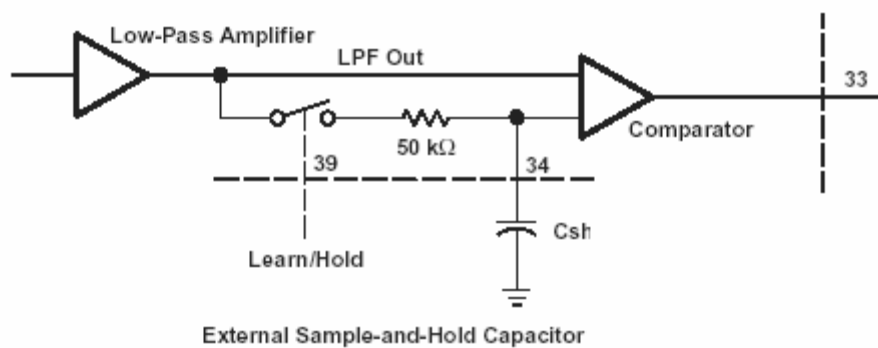


Figure 10: Data Slicer

2.3 Serial Interface

The TRF6901 is controlled through a serial interface; there are four 24-bit control words (A, B, C, D) which set the device state. The A and B words are almost identical and provide configuration settings for two modes, designated 0 and 1, commonly used to configure transmit and receive states. The C word sets the various clock dividers. The D word is used to trim the external crystal frequency and tune the demodulator [3].

2.3.1 Clock Output Buffer

The clock-output buffer is provided to use the TRF6901 crystal oscillator to drive an external microcontroller (MCU) or other base-band device, eliminating the need for a second clock circuit.

2.4 Designing an application with TRF6901

Wireless transceiver designs can be simple or complex based upon the performance and design complexity. Usually, simple designs are characterized by low data rate, low cost and short transmission ranges (under 100m). Complex designs include higher data rates for longer

transmission ranges (over 100m). While designing an application, the following three factors are required be considered.

2.4.1 Data Rate

Data rate plays an important role in determining the loop filter bandwidth, lock time and phase noise. TRF6901 is designed to support data rate 2.4 to 94 kbps for normal operation in 2-FSK without including the training sequences, error correction or other overhead [4].

2.4.2 Data Coding

Pulse code modulation (PCM) technique is usually employed for baseband coding. It is the name given to the class of baseband signals obtained from a digital word [7]. The source information is sampled and quantized to one of the L levels. Then each quantized sample is digitally encoded into an l-bit ($l = \log_2 L$) codeword. During baseband transmission the codeword bits are transformed to pulse waveform. The various PCM waveforms are illustrated in figure 11 and described in Table 2 [7].

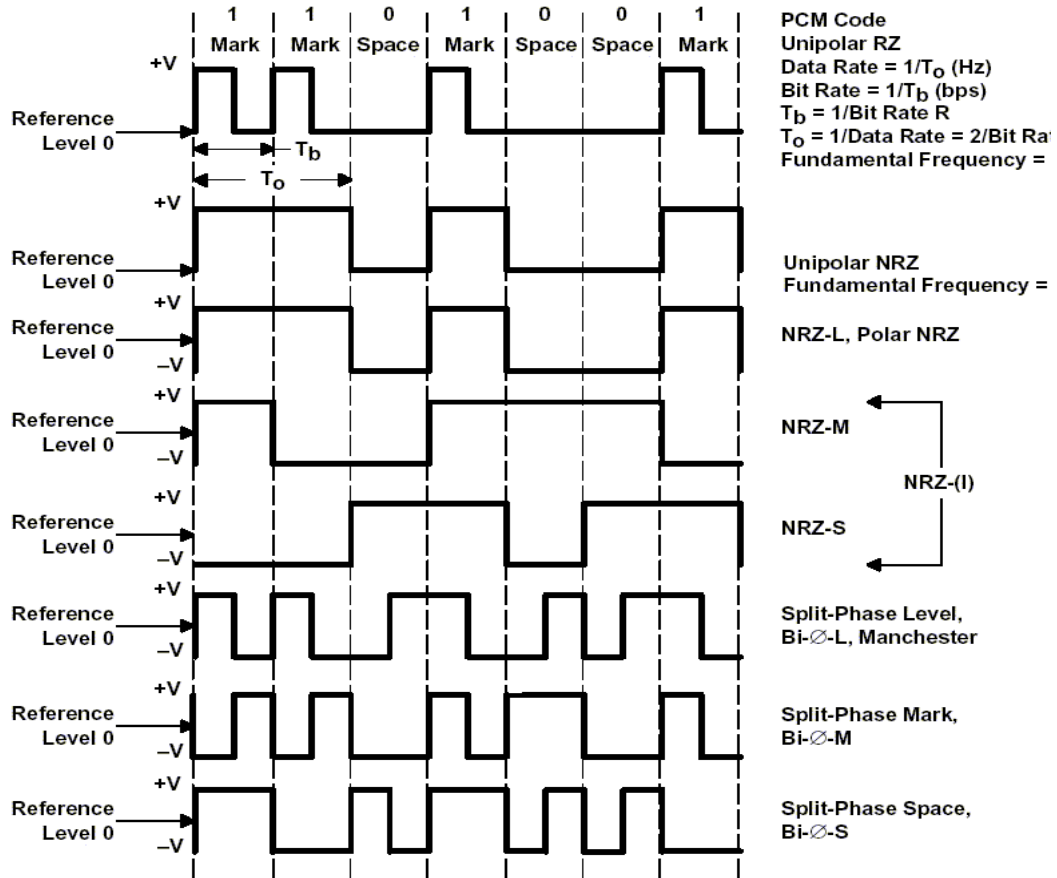


Figure 11: Common digital base band encoding schemes

Table 2: PCM Binary Coding Methods

PCM Code Type	RZ (Return Zero)	NRZ (Non-Return Zero)	Phase Encoded	Ref. Level	Transitions
Unipolar RZ	X			0 level	Change of state from 0 to 1, and a 1/2-bit period
Unipolar NRZ		X		0 level	Change of state from 0 to 1 or from 1 to 0
NRZ-L (level)		X		Center of pulse	Change of state from 0 to 1 or from 1 to 0
NRZ-M (Mark)		X		Center of pulse	1 or mark is represented by a change in level, 0 or space is represented by no change in level
NRZ-S (Spaced)		X		Center of pulse	0 or space is represented by a change in level, 1 or mark is represented by no change in level
Bi- ϕ -Level, Manchester			X	Center of pulse	A 1 is represented by a 1/2-bit pulse at the start of the bit interval. A 0 is represented by a 1/2-bit pulse at the end of the bit interval
Bi- ϕ -Mark (Mark)			X	Center of pulse	Transition occurs at the beginning of each bit interval 1 is represented by a second transition 1/2-bit later. 0 is represented by no second transition 1/2-bit later.
Bi- ϕ -Space (Space)			X	Center of pulse	Transition occurs at the beginning of each bit interval 0 is represented by a second transition 1/2-bit later. 1 is represented by no second transition 1/2-bit later.

The choice of coding scheme has important implications for several parts of the transceiver design, including loop filter bandwidth, frequency deviation, and operating the TRF6901 in learn and hold modes. Systems with low data rates (2.4 kbps to around 30 kbps) are often implemented with Manchester coding. Systems with data rates higher than 30 kbps are often implemented with unipolar NRZ (non-return-to-zero) coding [4].

2.4.3 FSK Modulation Theory

Binary FSK is a modulation scheme used to send digital data by shifting the frequency of a continuous carrier in a binary manner to one or the other discrete frequencies [9]. One frequency is designated as “mark”, corresponding as a binary 1 and the other as “space”, corresponding as a binary 0 as shown in Figure 12.

The FSK signal is mathematically represented by,

$$s(t) = A_c \times \cos(\omega_c t + k_f \times \int_{-\infty}^t m(\alpha) d\alpha)$$

where, k_f is frequency modulation gain constant

A_c is the carrier amplitude

$m(\alpha)$ is the baseband signal

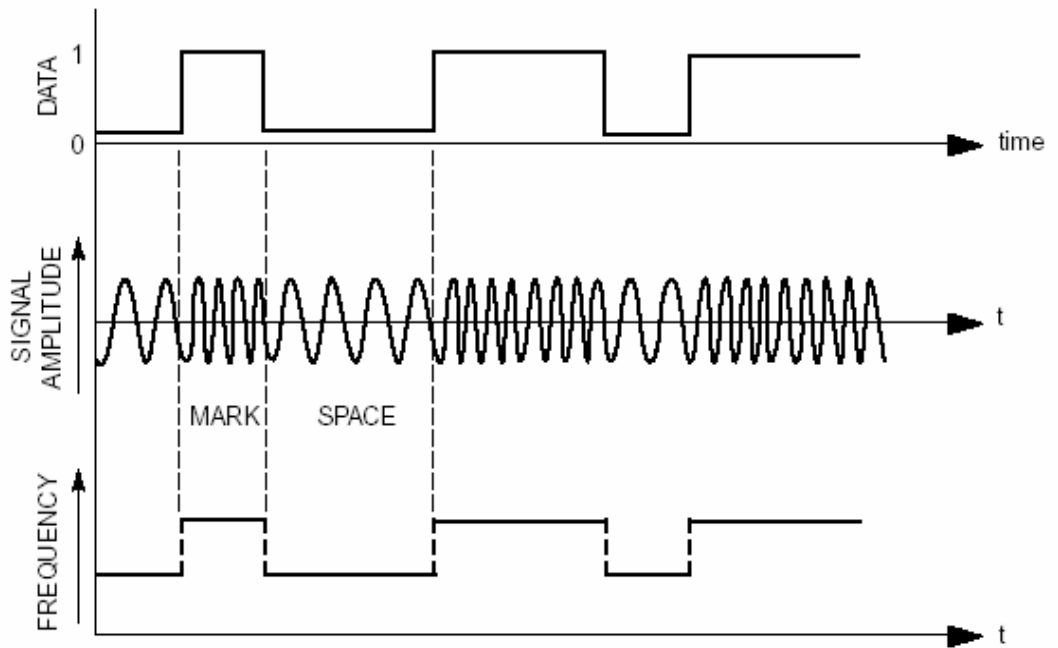


Figure 12: Binary FSK signal generation

2.5 Studied Module TRF6901/MSP430 Demonstration and Development Kit

The characterization and evaluation of the transceiver is done with reference to MSP-TRF6901-DEMO kit provided by the Texas Instruments. The board is shown in figure 13.

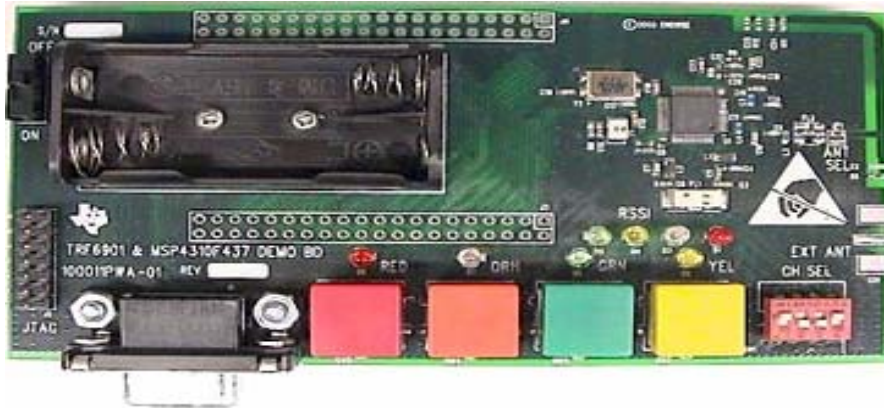


Figure 13: TRF6901/MSP430 Demonstration and Development kit

2.5.1 Hardware Overview

The kit consisting of two identical boards programmed to communicate using US ISM band frequency @ 915 MHz is used to demonstrate a bi-directional wireless link. Each board has a MSP430F449 microcontroller to provide the base band data and TRF6901 single-IC transceiver to perform radio frequency communication. The communication is half-duplex on the US ISM band @ 38.4 Kbps data rate employing NRZ base-band coding [10]. The kit employs an inverted F design on-board PCB antenna.

There are some provisions for the alternate configurations in the kit such as for an external antenna, a RS-232 serial link, a SAW filter, a MSP430 disable, an on-board LDO regulator and a high-frequency crystal.

2.5.1.1 MSP430F449

MSP430F449 is one of the popular mixed-signal microcontrollers produced by Texas Instruments. MSP40F449 features a powerful 16-bit RISC(Reduced Instruction Set Computing), 16-bit registers and constant generators with two built-in 16-bit timers, a fast 12-bit A/D converter, two USART (Universal serial synchronous asynchronous communication interfaces), 48 I/O pins and a LCD (liquid crystal driver) with up to 160 segments. It includes 60 KB + 256 B Flash Memory and 2 KB RAM and operates in five power saving modes [11]. Figure 14 shows a functional block diagram of the MSP430F449.

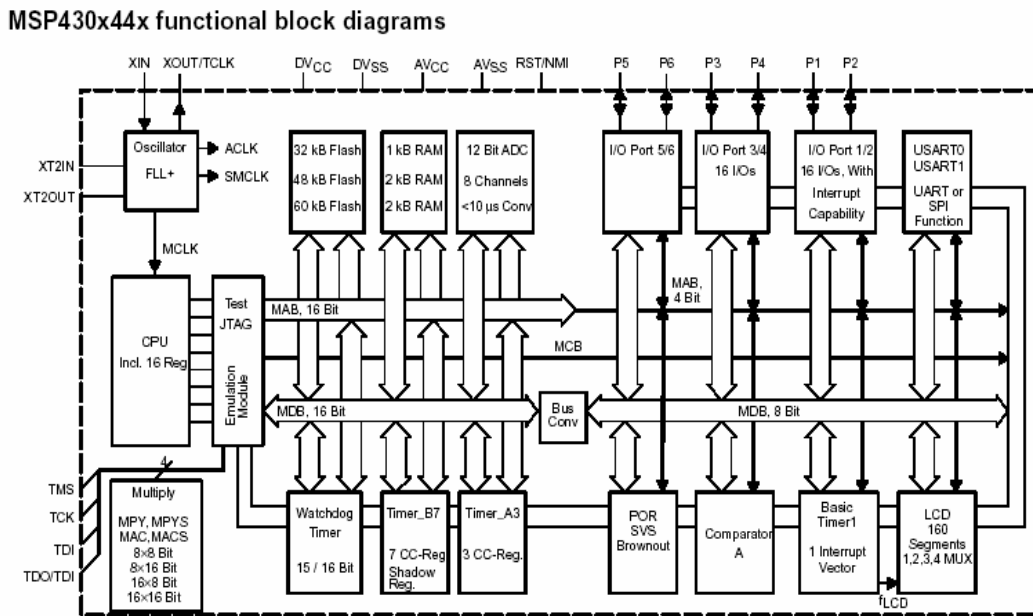


Figure 14: MSP430x44x functional block diagram

2.5.1.2 Embedded Antenna

The MSP-TRF6901-DEMO kit provided by the TEXAS INSTRUMENTS employs an inverted-F design PCB antenna where one short leg of the antenna is shorted to ground and the longer end is open or tuned with parallel RC termination to ground. The resistor and capacitor values are adjusted to optimize the performance of the antenna. The antenna has a poor return loss around 1.8 GHz so that will help attenuate the radiated power second harmonic.

The short arm of the antenna is 60 mils wide and 315 mils long, measuring from the center of the feed point (on the antenna itself) to the end of the terminating component footprints where a zero ohm resistor is installed with capacitor empty.

The long arm of the antenna is 60 mils wide and 1410 mils long, measuring from the center of the feed point, along the midline to the end of the most distant terminating component footprint. Both arms are separated from the near-side ground plane by 67 mils. The termination of the long arm is a parallel RC circuit, 1K and 0.5 pF. The lower ground plane is tied to the upper ground plane by vias located close to the edge of the ground plane and spaced every 100 to 200 mils. The substrate is 0.062 FR4 with dielectric constant 4.3.

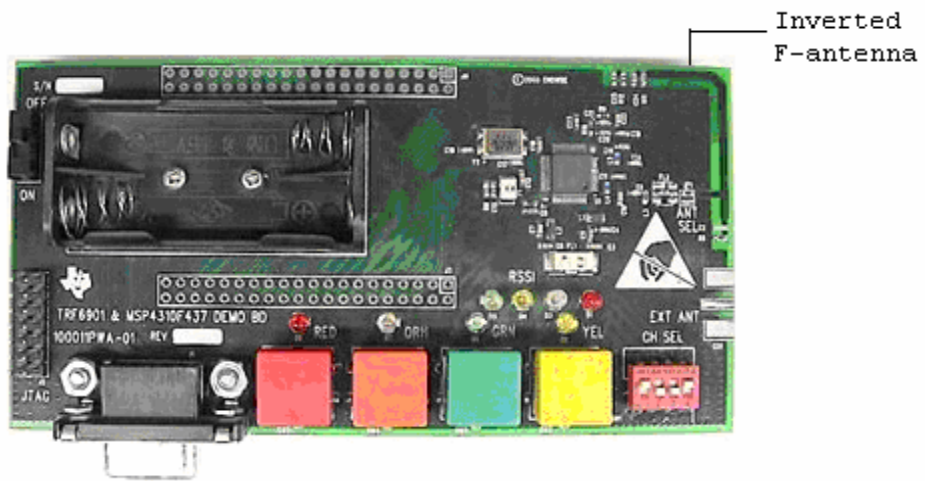


Figure 15: MSP-TRF6901 Demo kit

3 RANGE ESTIMATION

The focus of this thesis is on the characterization and performance analysis of a wireless transceiver. Communication range is a very important parameter which characterizes a wireless link. It is always difficult to predict the range. The vagaries of RF propagation depend on numerous factors such as multi-path interference, inter-symbol interference, interference due to other stations especially in the unlicensed band and noise. Moreover, wireless applications designed for indoor propagation can be affected by obstructions and building materials, radiating devices, antenna orientations and mounting heights. Typically, the range measurements are performed in either strictly laboratory environment or the open field.

For the open field range testing, specifications such as the height above ground of transmitter, receiver, type of antenna and its orientation, operating conditions (handheld), criteria for successful communication (number of correct messages received per number of messages sent) must be considered. There are in fact other factors in the open field range testing such as ground conductivity, near vicinity reflecting objects, noise on the communication channel and incidental transmissions that cannot be controlled.

3.1 Factors determining range

Idea free-space propagation is governed by the Friis transmission formula, given as:

$$P_r = P_t * G_t * G_r * \left(\frac{\lambda}{4\pi d} \right)^2 \text{-----} (1)$$

where,

P_r is the received power in Watts

P_t is the transmit power in Watts

G_t is the transmit antenna gain

G_r is the receive antenna gain

λ is the wavelength in meters

d is the distance in meters

In wireless applications design, the effective communication range calculations take into consideration the following parameters.

3.1.1 Line-of-sight

In RF communication, the transmission medium being the atmosphere, the signal is exposed to a complex array of propagation conditions including potential ground reflections, rain attenuation, interference from other radio systems, and atmospheric effects that can result in performance impairments. The line-of-sight (LOS) is an effective and reliable transmission medium. It is the straight line connecting the transmitter and the receiver with no obstructions in between. It provides a limit on the range of a hypothetical RF link. The signal is strongest when the receiver has a LOS to the transmitter. The Fresnel zone is the area of a circle around the line of sight. The Fresnel zone is defined as:

$$R = \sqrt{\lambda \times D}$$

where,

R is the radius of the Fresnel zone in meters

λ is the wavelength in meters

D is the distance between sites in meters

When at least 80% of the first Fresnel zone is clear of obstacles, propagation loss is equivalent to free space loss [12].

3.1.2 Transmitter and Receiver Line Losses

The path followed by the RF energy, as it is sent to and from the antenna, is associated with a loss of power. This loss occurs because of the escape of energy through less than perfect shielding, resistance, and because of the reflection of energy as it passes through less than perfect shielding, resistance, and because of the reflection of energy as it passes through less than perfect line couplers. Line losses which occur in commonly used coaxial cables are quantified, and are published by the manufacturer. The best way to determine actual line loss is with an RF power meter inserted before and after the transmission line.

3.1.3 Power Output and Receiver Sensitivity

Transmitter output power is the power available at the transmitter. One of the major parameters used in analyzing the performance of radio frequency (RF)

communications links is the amount of transmitter power directed toward an RF receiver(s) by the antenna subsystems. This power is derived from a combination of transmitter power and the ability of the antenna to direct that power toward RF receiver.

Receiver sensitivity is the minimum amount of RF signal at the receiver input for certain performance (BER). It depends on the thermal noise power generated in the receiver expressed as noise figure, the noise bandwidth of the receiver, and the required output signal-to-noise ratio [1]. It can be expressed as follows:

$$(P_{\min})_{\text{dBm}} = (N_{\text{in}})_{\text{dBm}} + (\text{NF})_{\text{db}} + (10 \log_{10} B)_{\text{dB}} + (\text{Predetection S/N})_{\text{dB}}$$

where,

P_{\min} is the minimum signal power applied to the receiver input that gives a desired signal to noise ratio.

N_{in} is the available input noise power

NF is the noise figure

B is the bandwidth

S/N is the signal to noise ratio

3.1.4 Transmit and Receive Antenna Gain

Antennas are passive elements in an RF circuit and do not actually produce a gain of the RF power. However, antennas can be designed to focus the energy in a specific plane or pattern, thereby producing an effective gain in a particular direction as compared to a unidirectional antenna.

Antenna gain is a very important figure of merit of an antenna. Usually, there are two basic methods to measure the gain of the antenna, namely, absolute-gain and gain-transfer. The absolute gain method is used to calibrate antennas that can be further used as standard antennas for gain measurements. It doesn't require a prior knowledge of the antenna gains. The gain transfer method requires to be used in conjunction with standard gain antennas to determine the absolute gain of the AUT [12].

3.1.4.1 Absolute Gain Measurements

The absolute gain measurements method is based on the Friis transmission formula given in equation (1).

It can be expressed in logarithmic decibel form as:

$$(G_t)_{\text{dB}} + (G_r)_{\text{dB}} = 20 \log_{10} \left(\frac{4\pi d}{\lambda} \right) + 10 \log_{10} \left(\frac{P_r}{P_t} \right)$$

where,

P_r is the received power in Watts

P_t is the transmit power in Watts

G_t is the transmit antenna gain in dB

G_r is the receive antenna gain in dB

λ is the wavelength in meters

d is the distance in meters

This method assumes that the measuring system employs two antennas separated by a distance 'd' satisfying the far field criteria of each antenna.

3.1.4.2 Gain - Transfer Measurements

It is the most common method employed to measure the gain of the antenna. This method utilizes a standard antenna with known gain to determine the absolute gain of the AUT.

This method requires two sets of measurements. In the first set, the AUT is made as a receiving antenna and the received power (P_T) is recorded. In the other set, the AUT is replaced by a standard antenna and the received power is recorded (P_S). The experimental set up is maintained intact with the same input power maintained on both sets. For free space calculation, the gain of the antenna is given by,

$$(G_T)_{\text{dB}} = (G_S)_{\text{dB}} + 10 \log_{10} \left(\frac{P_T}{P_S} \right)$$

3.1.5 Path loss

Path loss is the significant amount of attenuation of the electromagnetic energy propagating through space. The free space attenuation of RF signals is calculated using the free space path loss formula.

$$P_{\text{loss}} = \left(\frac{4\pi d}{\lambda} \right)^2$$

where, λ is the wavelength of the RF signal and d is the distance of propagation.

More simply, it can be expressed logarithmically in decibels as:

$$P_{loss} = 32.4 + 20 \log_{10} d + 20 \log_{10} f$$

where,

32.4 is the reference constant

D is the distance in kilometers

f is the frequency in MHz

Shown below in figure 15 is the free space path loss as a function of distance @ 915 MHz.

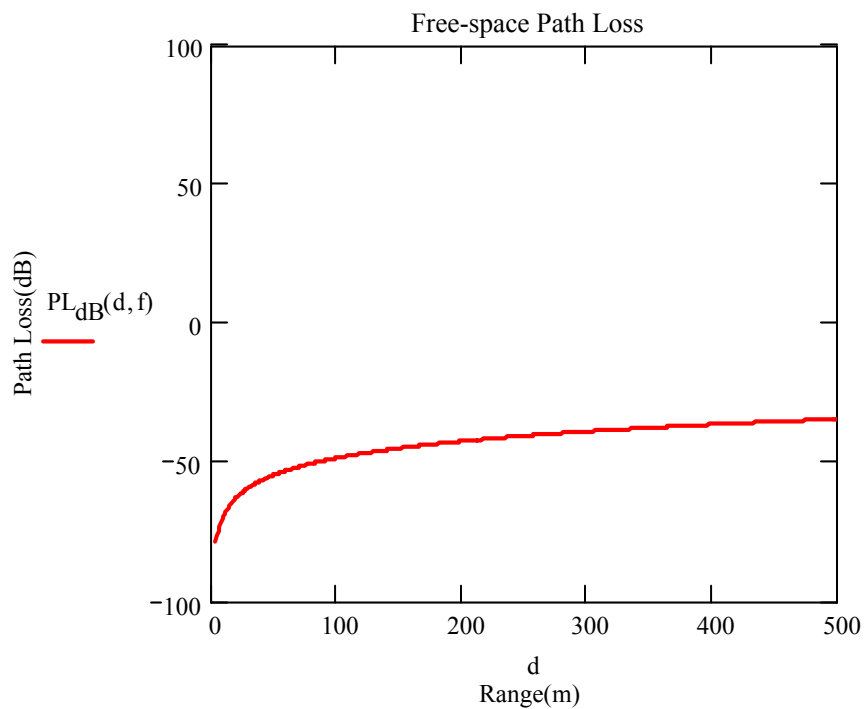


Figure 16: Free space path loss as a function of distance @ 915 MHz

3.2 Experiments on Range

3.2.1 Antenna measurements

The antenna is a transducer between the controlled energy residing within the system and the radiating energy existing in free space. A good antenna design is required to realize good range performance. The principal properties of an antenna such as input impedance, polarization, gain, directivity, radiation efficiency, radiation pattern etc., doesn't depend on the transmitting or receiving method. The popular reciprocity theorem is also applicable to electromagnetic theory. It states that the power transferred between two antennas is same, regardless of which is used for transmission or reception, if the generator and load impedances are conjugates of the transmitting and receiving antenna impedances in each case [12].

3.2.1.1 Determination of the antenna pattern of the on-board PCB antenna

Antenna pattern measurement determines the radiation pattern of an antenna under test (AUT). It gives the relative magnitude and phase of an electromagnetic signal received from the AUT as a function of directional coordinates [4]. The properties of an antenna such as antenna pattern, gain etc., are always referenced to the far field region of the antenna. Though the measured field levels vary in the far field free space condition, the antenna pattern and the gain remains the same. The far field region is dominant at higher frequencies where the separation

distance $r > 2 D^2 / \lambda$, D being the largest dimension of the radiating object, λ being the wavelength.

3.2.1.1.1 Instruments Used

Following table 3 lists the test equipments used for the gain and pattern measurement of the antenna.

Table 3: Instruments Used

Model	Description
Wiltron Programmable Sweep Generator, 6647A	<ul style="list-style-type: none"> • Frequency range: 10 MHz -18.6 GHz <ul style="list-style-type: none"> • Output power <ul style="list-style-type: none"> ✓ Internally leveled maximum (dBm):>10 <ul style="list-style-type: none"> • Frequency Accuracy <ul style="list-style-type: none"> ✓ CW Mode (MHz): ± 10 ✓ Sweep Mode ≤ 50 MHz: ± 15 • Sweep Time: 0.01 to 99 seconds <ul style="list-style-type: none"> • Sweep Modes: <ul style="list-style-type: none"> ✓ Full Sweep ✓ F1 to F2 Sweep ✓ M1 to M2 Sweep ✓ Delta F F0 Sweep ✓ Delta F F1 Sweep • Markers: Video, RF, Intensity • Leveling Modes: Internal, Detector, Power Meter
Wiltron 560 A Network Analyzer	<ul style="list-style-type: none"> • Frequency range: 1 MHz-34 GHz <ul style="list-style-type: none"> • Channels: Three (A, B, R) • Dynamic measurement range and sensitivity <ul style="list-style-type: none"> ✓ A and B with detectors: +16 dBm to -50 dBm ✓ A and B with SWR Autotester: +16 dBm to 50 dBm ✓ R with Detector: +16 dBm to -30 dBm • Resolution: independent control for A and B in steps of 0.2, 0.5, 2.5, 10 dB per division

	<ul style="list-style-type: none"> • Store trace: stores displayed traces in 1024 point memory
TRF6901 Demonstration and Development Kit	<ul style="list-style-type: none"> • US ISM band: 902 MHz to 920 MHz <ul style="list-style-type: none"> • NRZ coding scheme <ul style="list-style-type: none"> • FSK <ul style="list-style-type: none"> • 38.4 Kbs • On-board PCB antenna • TRF6901 and MSP430F449 components <ul style="list-style-type: none"> • JTAG connector <ul style="list-style-type: none"> • MSP430 and TRF6901 I/Os • SMA connector footprint for additional range
SWR Autotester 560-97NF50-1	<ul style="list-style-type: none"> • 38 dB directivity • Low test port reflections • Broadband 10 MHz to 18 GHz frequency range
RF Detector Wiltron Model 560-7N50	<ul style="list-style-type: none"> • 10 MHz to 18.5 GHz frequency range <ul style="list-style-type: none"> • +20 dBm Max <ul style="list-style-type: none"> • 50 ohm
Yagi Antenna	<ul style="list-style-type: none"> • 750 MHz to 1.25 GHz frequency range

3.2.1.1.2 Testing Method

The single axis rotational pattern technique was employed for the pattern measurement of the PCB antenna. The AUT, i.e., the TRF6901 demonstration and development kit configured in

transmitting mode was placed on a rotational positioner and rotated about the azimuth to generate a two dimensional polar pattern. The measurement was accomplished by using a Yagi antenna as a measuring antenna (MA). Figure 17 shows a typical test set up.

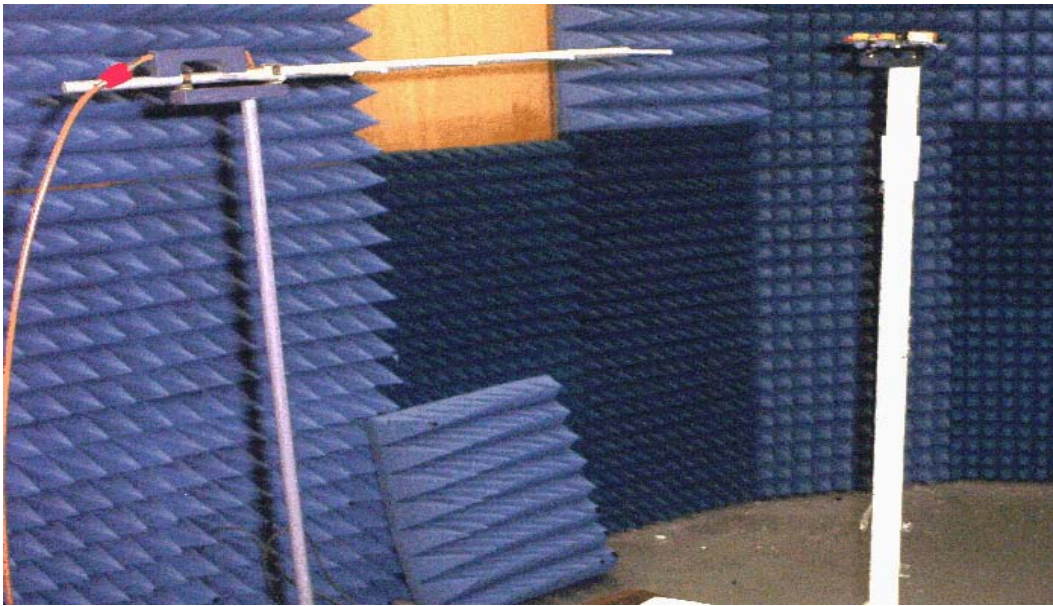


Figure 17: Experimental Setup of on board PCB antenna of TRF6901 Demonstration and Development kit configured in transmitting mode and a yagi antenna in receiving mode.

The AUT (transmitter) is placed in a positioner above ground, and a Yagi antenna is placed in level with the AUT at a fixed distance. The MA is connected to the 560A Network Analyzer as in receiving mode. The transmitter is rotated every 10° and the reading of the power level is noted when the antenna is tuned to achieve maximum radiated power. The reading is

taken for 360° rotations and the response between the antennas is measured as the function of angle. These measurements were performed in an anechoic environment, Microwave and Antenna Measurements Laboratory, University of Central Florida. The measurements were done with extreme care, minimizing the reflections from the surrounding objects, pertaining to ± 0.2 discrepancies.



Figure 18: Short bursts of data pulses received by the MA shown in Wiltron 560A Network Analyzer

3.2.1.1.3 Experimental Results

3.2.1.1.3.1 Experiment 1

Figure 19 shows a typical experimental setup. Both the antennas are placed in horizontal position 1.83 meters apart 87 cm above the ground. Figure 20 shows the measured data. Table 4 contains the measured data.

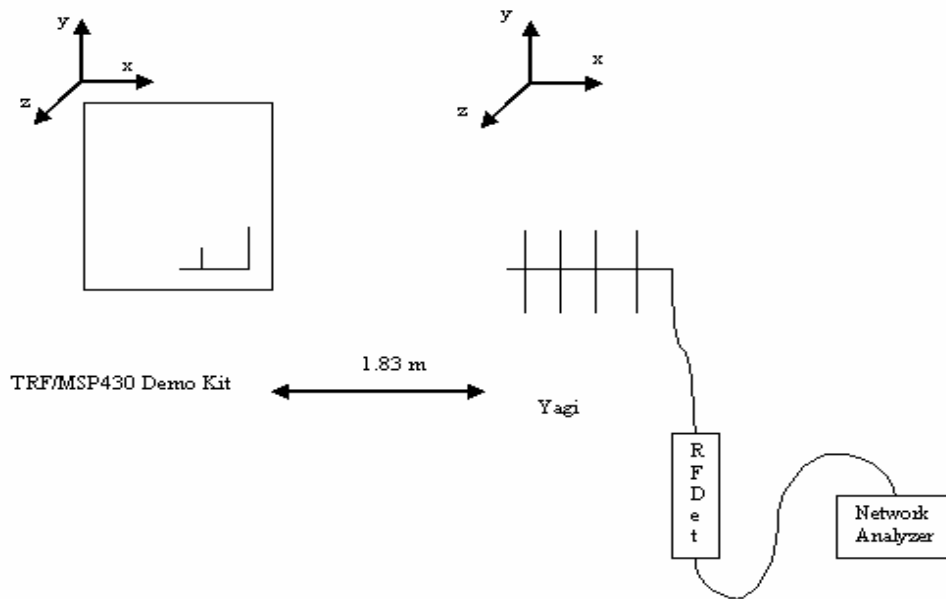


Figure 19: Experimental Setup

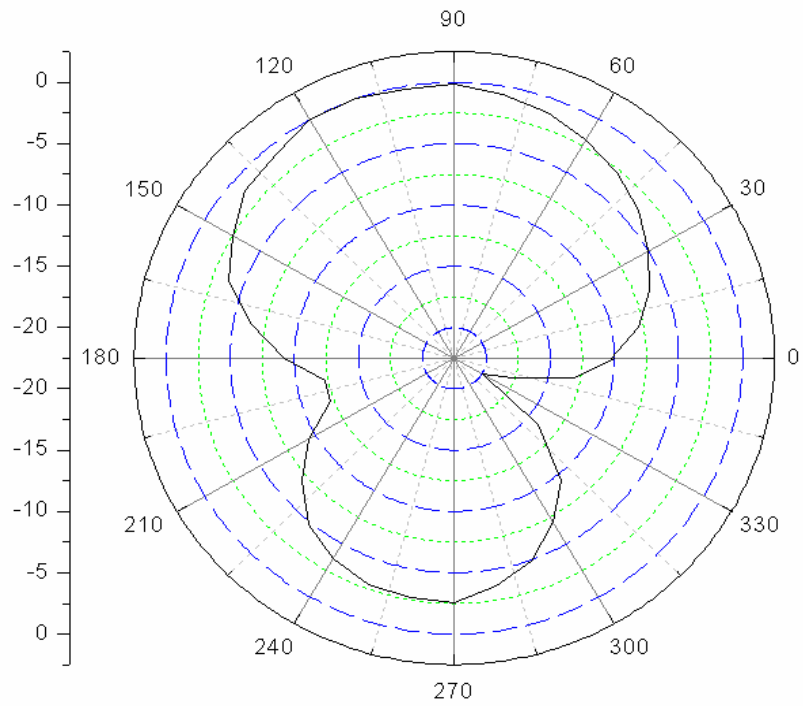


Figure 20: Horizontal Polarization of the embedded antenna

Table 4: Horizontal Polarization data referred to experiment 1

Angle(deg)	Normalized Data (dB)	Actual Data(dB)	Angle(deg)	Normalized Data (dB)	Actual Data(dB)
0	-10.2	-46.8	180	-9.2	-45.8
10	-7.9	-44.5	190	-12.2	-48.8
20	-6.3	-42.9	200	-12.2	-48.8
30	-5	-41.6	210	-9.4	-46
40	-3.7	-40.3	220	-6.9	-43.5
50	-2.8	-39.4	230	-4.8	-41.4
60	-2	-38.6	240	-3.6	-40.2
70	-1.2	-37.8	250	-2.9	-39.5
80	-0.7	-37.3	260	-2.7	-39.3
90	-0.2	-36.8	270	-2.6	-39.2
100	-0.2	-36.8	280	-3.6	-40.2
110	0	-36.6	290	-4.9	-41.5
120	0	-36.6	300	-7	-43.6
130	-0.8	-37.4	310	-9.5	-46.1
140	-1.2	-37.8	320	-14	-50.6
150	-2.5	-39.1	330	-20	-56.6
160	-3.8	-40.4	340	-17.7	-54.3
170	-6.3	-42.9	350	-13.1	-49.7
			360	-9.9	-46.5

3.2.1.1.3.2 Experiment 2

Both the antennas are placed in vertical position, 84 cm apart and 87 cm above the ground. Figure 21 shows a typical experimental set up. Figure 22 shows the measured data.

Table 5 contains the measured data.

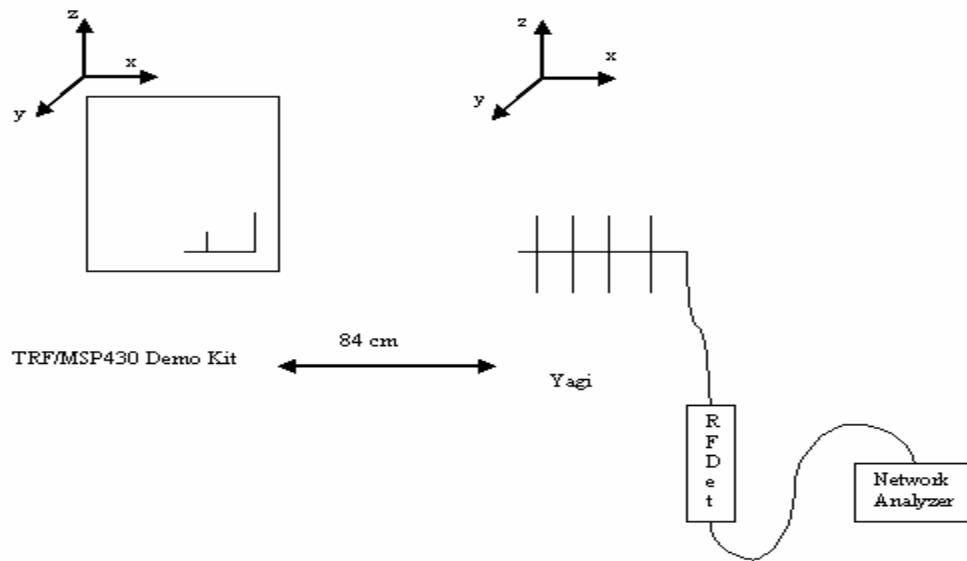


Figure 21: Experimental Setup

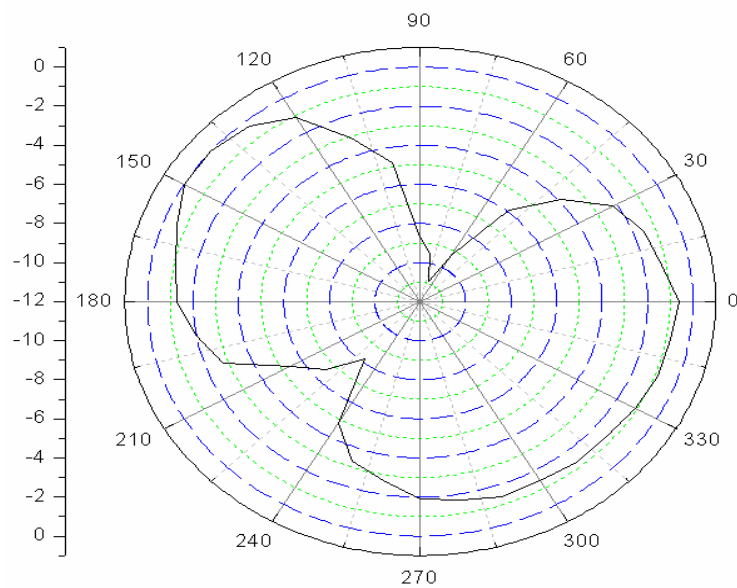


Figure 22: Vertical Polarization of the embedded antenna

Table 5: Vertical Polarization data referred to experiment 2

Angle(deg)	Normalized Data (dB)	Actual Data(dB)	Angle(deg)	Normalized Data (dB)	Actual Data(dB)
0	-0.6	-40.2	180	-40.9	-1.3
10	-1.2	-40.8	190	-41.6	-2
20	-1.5	-41.1	200	-42.4	-2.8
30	-2.2	-41.8	210	-45	-5.4
40	-3.9	-43.5	220	-46.2	-6.6
50	-5.9	-45.5	230	-47.8	-8.2
60	-9.2	-48.8	240	-44.4	-4.8
70	-10.9	-50.5	250	-42.9	-3.3
80	-9.5	-49.1	260	-42.3	-2.7
90	-8.7	-48.3	270	-41.5	-1.9
100	-4.8	-44.4	280	-41.3	-1.7
110	-3.1	-42.7	290	-41	-1.4
120	-1.1	-40.7	300	-41	-1.4
130	-0.3	-39.9	310	-40.9	-1.3
140	0	-39.6	320	-40.9	-1.3
150	0	-39.6	330	-40.7	-1.1
160	-0.6	-40.2	340	-40.5	-0.9
170	-1.1	-40.7	350	-40.4	-0.8
			360	-40.2	-0.6

3.2.1.1.3.3 Experiment 3

Figure 23 shows a typical experimental set up for the cross-polarization pattern measurement. The TRF board is in horizontal position with the Yagi antenna in vertical position separated by a distance of 84 cm and 87 cm above the ground. Table 6 contains the measured data.

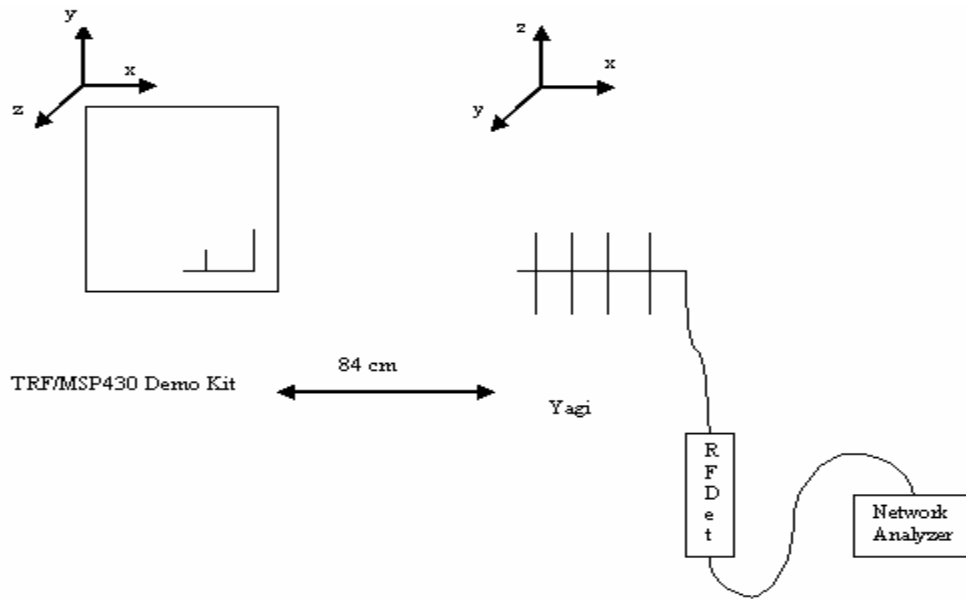


Figure 23: Experimental Set up

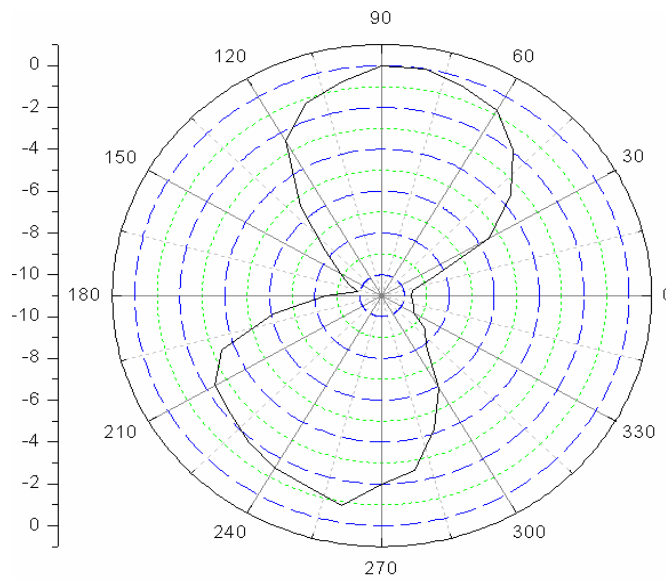


Figure 24: Cross-polarization pattern

Table 6: Cross-polarization data referred to experiment 3

Angle(deg)	Normalized Data (dB)	Actual Data(dB)	Angle(deg)	Normalized Data (dB)	Actual Data(dB)
0	-9.7	-61.3	180	-8.5	-60.1
10	-9.6	-61.2	190	-6.1	-57.7
20	-8.7	-60.3	200	-3.4	-55
30	-5.5	-57.1	210	-2.4	-54
40	-3.5	-55.1	220	-2.2	-53.8
50	-1.9	-53.5	230	-1.8	-53.4
60	-0.8	-52.4	240	-1.5	-53.1
70	-0.4	-52	250	-1.3	-52.9
80	0	-51.6	260	-0.8	-52.4
90	0	-51.6	270	-2	-53.6
100	-0.6	-52.2	280	-2.5	-54.1
110	-1.2	-52.8	290	-4.2	-55.8
120	-2.4	-54	300	-5.9	-57.5
130	-5.4	-57	310	-7.9	-59.5
140	-7.7	-59.3	320	-8.5	-60.1
150	-8.9	-60.5	330	-9.4	-61
160	-9.4	-61	340	-9.5	-61.1
170	-9.9	-61.5	350	-9.6	-61.2
			360	-9.7	-61.3

3.2.1.1.3.4 Experiment 4

Figure 25 shows a typical experimental set up. The TRF board is in vertical position with the Yagi antenna in horizontal position separated by a distance of 86cm and 87 cm above the ground. Figure 26 shows the measured data. Table 7 contains the measured data.

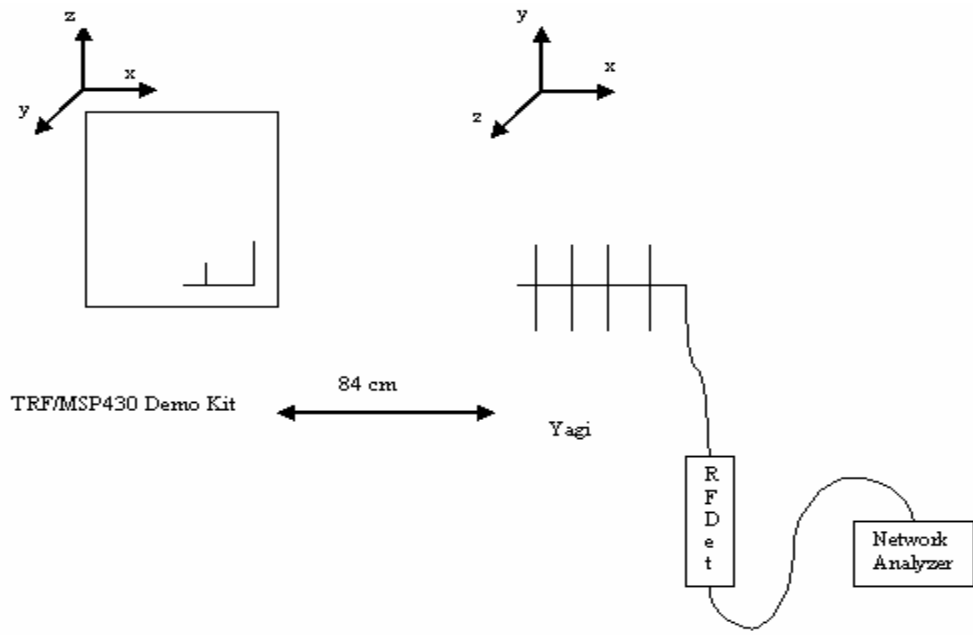


Figure 25: Experimental Set up

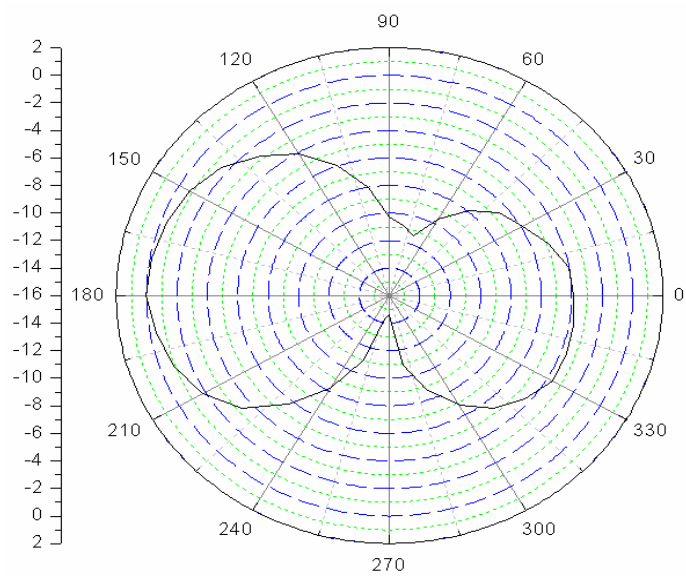


Figure 26: Cross-polarization pattern

Table 7: Cross-polarization data referred to experiment 4

Angle(deg)	Normalized Data (dB)	Actual Data(dB)	Angle(deg)	Normalized Data (dB)	Actual Data(dB)
0	-3.9	-50.1	180	0	-46.2
10	-4	-50.2	190	-0.4	-46.6
20	-4.9	-51.1	200	-0.9	-47.1
30	-5.9	-52.1	210	-1.8	-48
40	-6.6	-52.8	220	-3.3	-49.5
50	-7.9	-54.1	230	-5.7	-51.9
60	-9.6	-55.8	240	-8.2	-54.4
70	-11.4	-57.6	250	-11	-57.2
80	-10.8	-57	260	-14.3	-60.5
90	-10.3	-56.5	270	-14.6	-60.8
100	-8	-54.2	280	-10.9	-57.1
110	-5.9	-52.1	290	-8.7	-54.9
120	-4.1	-50.3	300	-6.8	-53
130	-2.8	-49	310	-5.3	-51.5
140	-1.5	-47.7	320	-4.4	-50.6
150	-0.8	-47	330	-3.6	-49.8
160	-0.4	-46.6	340	-3.6	-49.8
170	-0.1	-46.3	350	-3.7	-49.9
			360	-3.9	-50.1

3.2.1.1.3.5 Experiment 5

Figure 27 describes the experimental set up. The TRF board is in vertical position with the Yagi antenna in horizontal position separated by a distance of 86 cm and 87 cm above the ground.

Figure 28 shows the measured pattern. Table 8 contains the measured data.

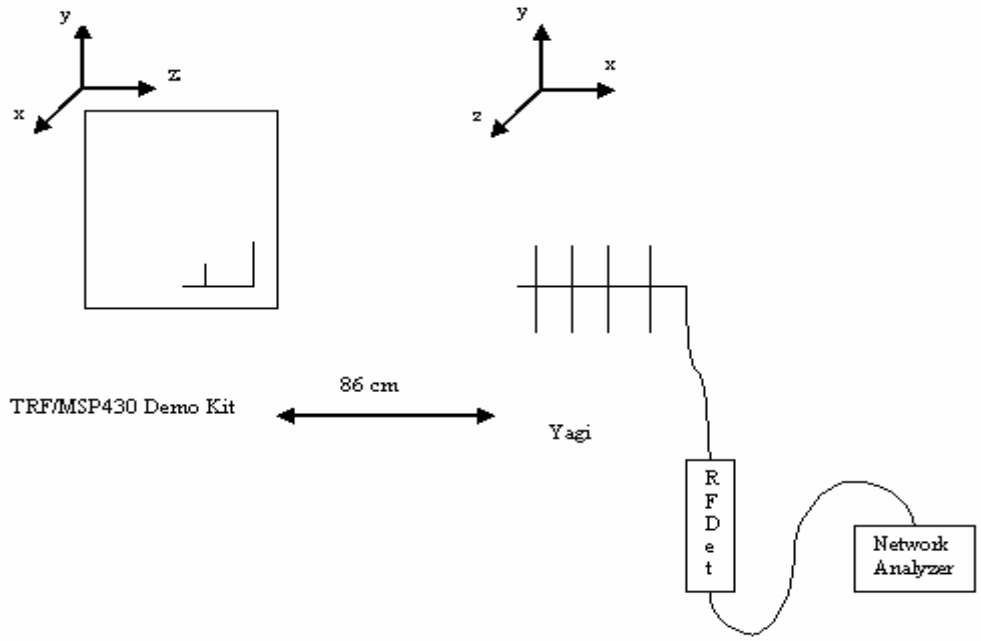


Figure 27: Experimental Set up

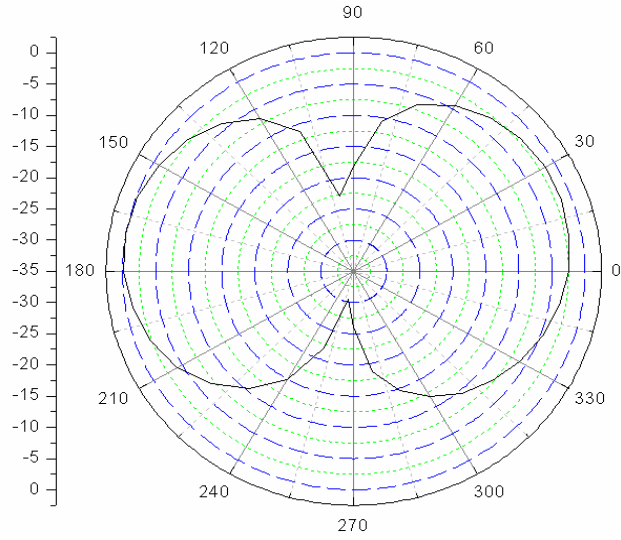


Figure 28: Cross-polarization pattern

Table 8: Cross-polarization data referred to experiment 5

Angle(deg)	Normalized Data (dB)	Actual Data(dB)	Angle(deg)	Normalized Data (dB)	Actual Data(dB)
0	-2.5	-32.7	180	-0.2	-30.4
10	-1.9	-32.1	190	-1	-31.2
20	-1.5	-31.7	200	-2.3	-32.5
30	-1.5	-31.7	210	-4.2	-34.4
40	-2	-32.2	220	-6.9	-37.1
50	-2.8	-33	230	-10.4	-40.6
60	-4.3	-34.5	240	-15	-45.2
70	-6.6	-36.8	250	-21.9	-52.1
80	-10.6	-40.8	260	-30.5	-60.7
90	-18.1	-48.3	270	-26	-56.2
100	-22.7	-52.9	280	-18.6	-48.8
110	-11.2	-41.4	290	-14.6	-44.8
120	-6.8	-37	300	-11.8	-42
130	-4.1	-34.3	310	-9.5	-39.7
140	-2.2	-32.4	320	-7.7	-37.9
150	-1	-31.2	330	-6.1	-36.3
160	-0.2	-30.4	340	-4.6	-34.8
170	0	-30.2	350	-3.4	-33.6
			360	-2.5	-32.7

3.2.1.2 Determination of the gain of TX and RX on-board PCB antenna

To measure the gain of the TX and RX antenna, the absolute gain method was employed. Due to the absence of a perfect anechoic chamber, there was a need for a directional antenna. First the gain of the directional antenna was measured, then all the pattern measurements carried out throughout this analysis was done with respect to the directional antenna, a Yagi. The gain of the embedded antenna was measured in the following three steps.

Step 1: Determination of the gain of the Yagi antenna

The gain of the Yagi antenna was calculated by the absolute gain method. First, an electromagnetic field was set up with the two standard calibrated dipole antennas. The received power was recorded. Then, one of the dipole was replaced by a Yagi antenna in the transmitting mode. The test was carried out for a distance of 1.83 meters with both the antennas placed 87 cm above ground. One of the dipoles with 2.54 dBi gain was set up as a receiving antenna and the received power shown in the network analyzer was recorded. The network analyzer was calibrated and a zero dBm reference was set. The received power was seen to be -18.2 dB down the reference. The experimental setup is shown in figure 29(a), (b).

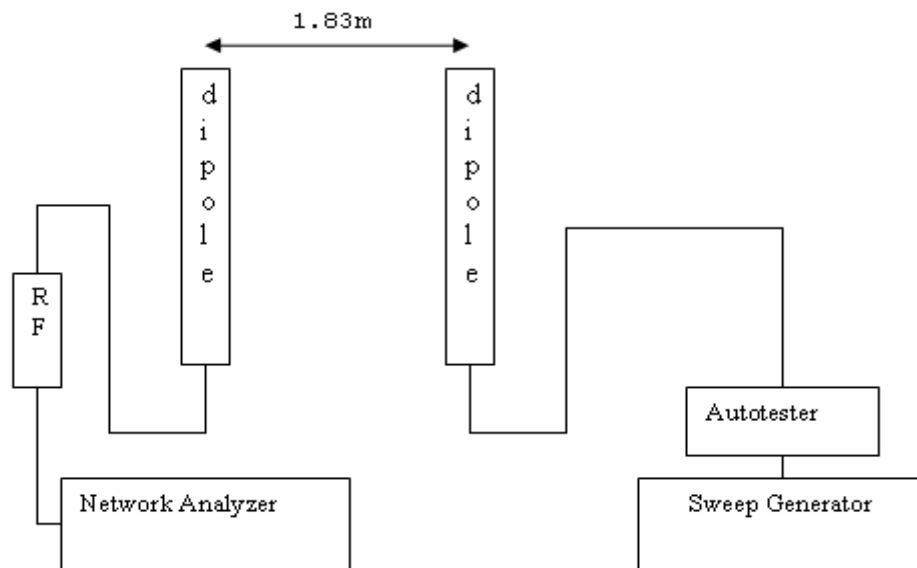


Figure 29(a) Experimental Set up for the gain measurement of the Yagi antenna

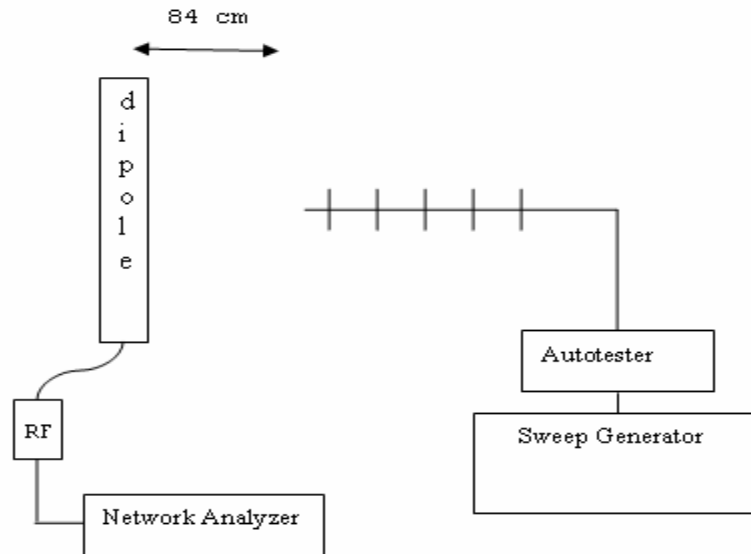


Figure 29 (b) Experimental Setup for determining the gain of the Yagi antenna

From this experimental setup the gain of the Yagi antenna was calculated to be 8.2 dBi.

Step 2: Record of Power Received by the standard dipole with Yagi in transmitting mode

To minimize the reflections in the anechoic chamber, the distance between the Yagi and a standard dipole antenna was reduced to 84 cm. The received power by the dipole antenna was recorded to be -18.4 dB down the zero dBm reference.

Step 3: Replacement of standard dipole with Yagi in receiving mode and embedded antenna in transmitting mode

The dipole antenna was replaced by the TRF/MSP430 antenna in the transmitting mode. The received power was recorded to be -26.4dB down the zero dBm reference. Figure 30 shows the experimental set up.

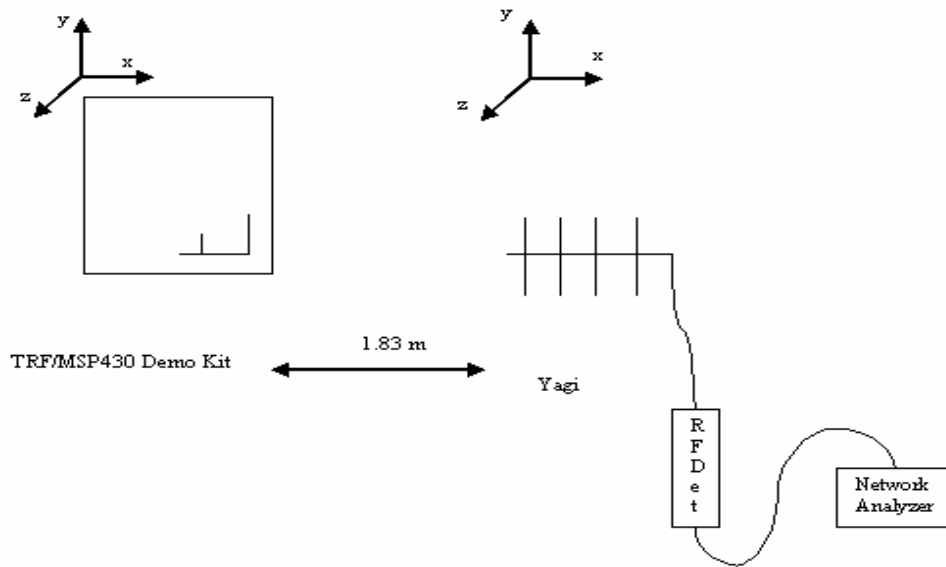


Figure 30: Experimental Setup for determining the gain of the embedded antenna

Substituting the given parameters in equation 1 the gain of the embedded antenna was found to be around 5.45 dB worse than a dipole.

3.2.1.3 Pattern Measurement with external dipole

An external dipole antenna with 2.3 dBi gain was connected to the TRF/MSP board and the pattern measurements were performed. First the pattern of the dipole antenna was measured. Figure 31 shows the experimental set up. The Yagi antenna was kept in transmitting mode at a

distance of 84 cm from the dipole in receiving mode. Figure 32 shows the measured pattern data.

Table 9 contains the measured data.

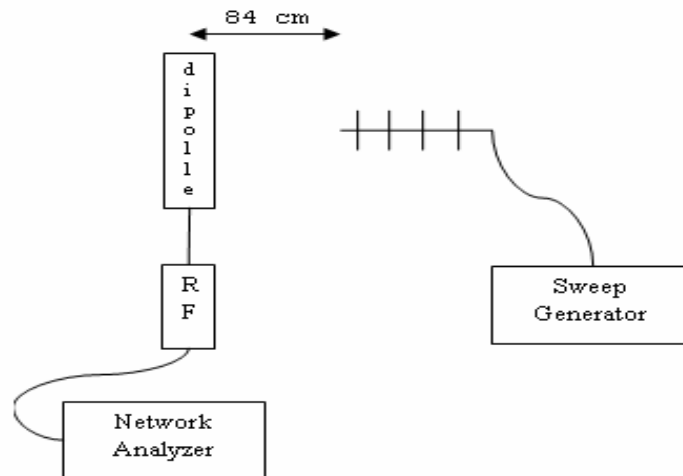


Figure 31: Experimental Setup

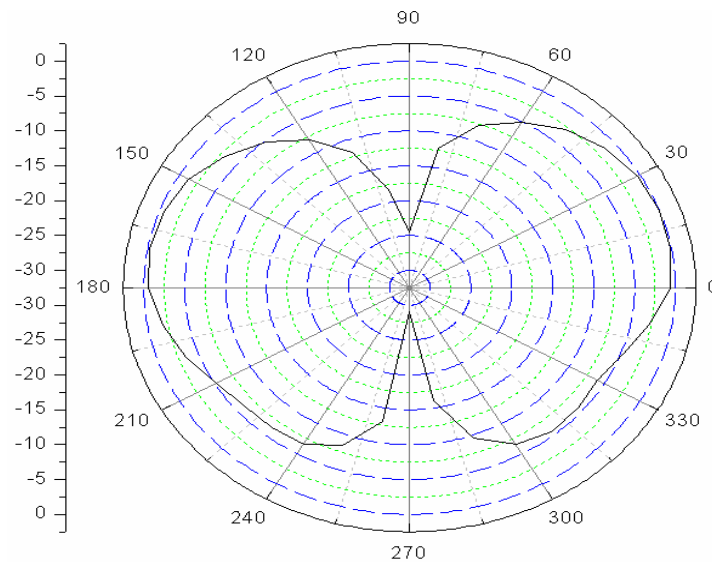


Figure 32: Measured pattern data of external dipole antenna

Table 9: External dipole horizontal polarization data without connecting to TRF6901 board

Angle(deg)	Normalized Data (dB)	Actual Data(dB)	Angle(deg)	Normalized Data (dB)	Actual Data(dB)
0	-0.6	-18.6	180	1	-18.6
10	-0.1	-18.1	190	-1.9	-19.9
20	0	-18	200	-3.4	-21.4
30	-0.4	-18.4	210	-5.2	-23.2
40	-1.3	-19.3	220	-6.1	-24.1
50	-2.8	-20.8	230	-6.4	-24.4
60	-5.1	-23.1	240	-6.6	-24.6
70	-7.7	-25.7	250	-8.5	-26.5
80	-12.2	-30.2	260	-13.1	-31.1
90	-24.5	-42.5	270	-29	-47
100	-18.2	-36.2	280	-16	-34
110	-11.9	-29.9	290	-9.6	-27.6
120	-8	-26	300	-6.6	-24.6
130	-5.2	-23.2	310	-5.6	-23.6
140	-3.1	-21.1	320	-5.6	-23.6
150	-1.3	-19.3	330	-6	-24
160	-0.6	-18.6	340	-4.8	-22.8
170	-0.2	-18.2	350	-2.7	-20.7
			360	-0.6	-18.6

Secondly, the internal embedded antenna of the TRF/MSP430 board was replaced by the same dipole antenna with no change in the initial setup and the pattern was measured. Figure 34 shows the measured pattern data. Table 10 contains the measured data.

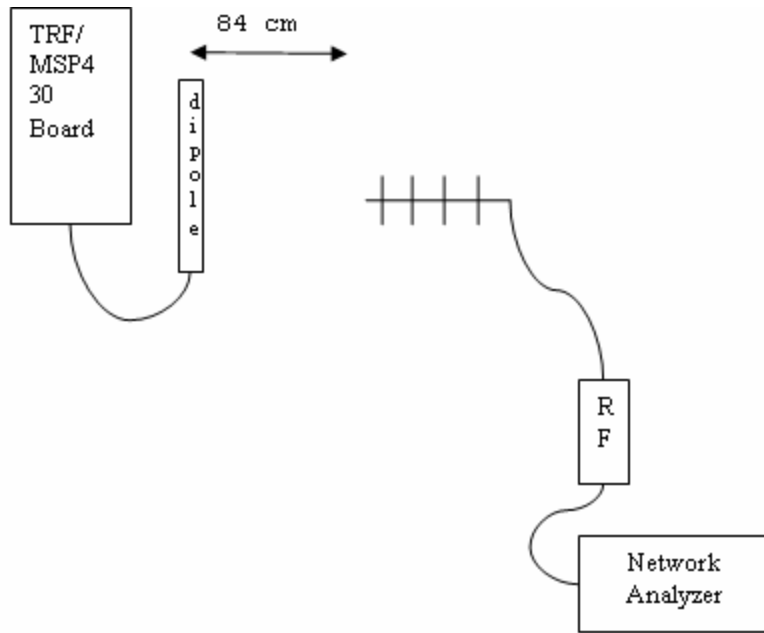


Figure 33: Experimental Setup

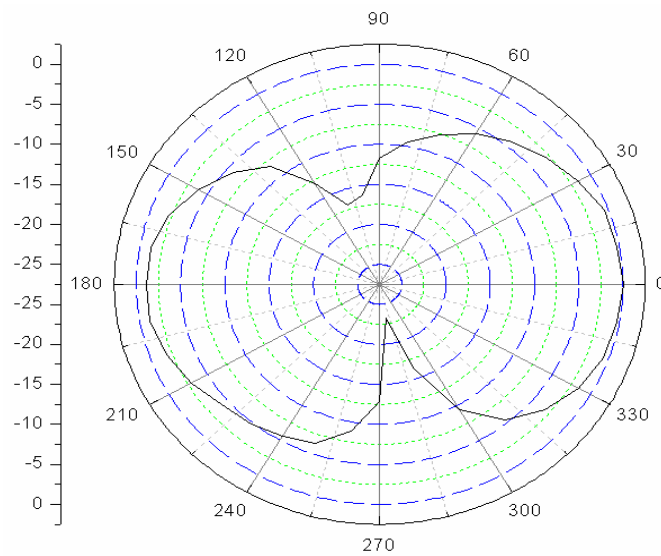


Figure 34: Measured pattern data of external dipole antenna connected to TRF/MSP430 board

Table 10: External dipole horizontal polarization data with connecting to TRF6901 board

Angle(deg)	Normalized Data (dB)	Actual Data(dB)	Angle(deg)	Normalized Data (dB)	Actual Data(dB)
0	0	-18.6	180	-1.1	-19.7
10	-0.3	-18.9	190	-1.1	-19.7
20	-0.5	-19.1	200	-1.9	-20.5
30	-1.7	-20.3	210	-2.9	-21.5
40	-2.9	-21.5	220	-4.2	-22.8
50	-4.2	-22.8	230	-4.8	-23.4
60	-5.8	-24.4	240	-5.6	-24.2
70	-7.6	-26.2	250	-6.4	-25
80	-9.5	-28.1	260	-8.9	-27.5
90	-11.8	-30.4	270	-12.8	-31.4
100	-16.2	-34.8	280	-23.2	-41.8
110	-16.9	-35.5	290	-16.4	-35
120	-13	-31.6	300	-9.4	-28
130	-8.3	-26.9	310	-5.4	-24
140	-5.8	-24.4	320	-3.2	-21.8
150	-3.8	-22.4	330	-1.6	-20.2
160	-2.1	-20.7	340	-0.6	-19.2
170	-1.3	-19.9	350	-0.3	-18.9
			360	0	-18.6

The gain of the dipole antenna was also found in the method followed previously. It was found out to be 2.15 dBi comparable to 2.3 dBi max given in the manufacturer's datasheet.

3.2.2 Power Measurements

3.2.2.1 Transmitted Power

The power transmitted by the TRF/MSP430 board was measured at the end of the SMA footprint. It was found out to be 4.4 dBm as opposed to 9 dBm given in the manufacturer's datasheet. The 4.6 dBm power degradation can be accounted for the use of common RF port with no switch. The power output was verified by measuring in the power meter also.

3.2.2.2 Receiver Sensitivity

The receiver sensitivity of the TRF6901 was measured with respect to the given TRF/MSP Demonstration kit. The experimental set up is described in Figure 35.

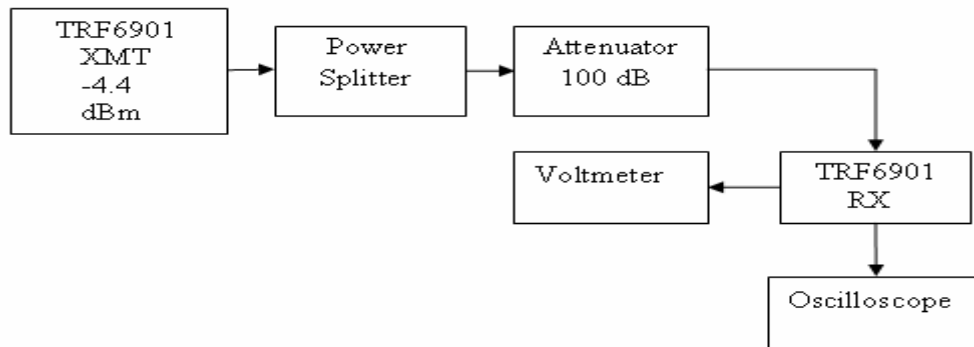


Figure 35: Experimental Setup for the receiver sensitivity measurement

The receiver sensitivity of the board was found to be -75 dBm.

3.2.3 Path loss

Path loss can be expressed logarithmically in decibels as:

$$P_{loss} = 32.4 + 20 \log_{10} d + 20 \log_{10} f$$

where,

32.4 is the reference constant

d is the distance in kilometers

f is the frequency in MHz

3.2.4 Link Distance Calculation

The following table summarizes the range calculation with all the given parameters.

Table 11: Link Calculation Results

PARAMETER	VALUE
Receiver Sensitivity, P_r	-75 dBm
Transmitted Power, P_t	4.4 dBm
Gain of the RX antenna, G_r	-5.45 dBi
Path loss, L_p	30.115 dB
Cable attenuation, C_t	0 dB
Gain of the TX antenna, G_t	-5.45 dBi
Frequency, f	915 MHz
Cable attenuation, C_r	0 dB
Link Range	69.75 meters

3.3 Simulation Results

With the provided dimensions of the antenna, the inverted F-antenna was simulated by using a commercial method of moment software packages IE3D from Zeland [4]. The highest meshing frequency was set up to 2.5 GHz with 20 cells per wavelength discretization and edge meshing.

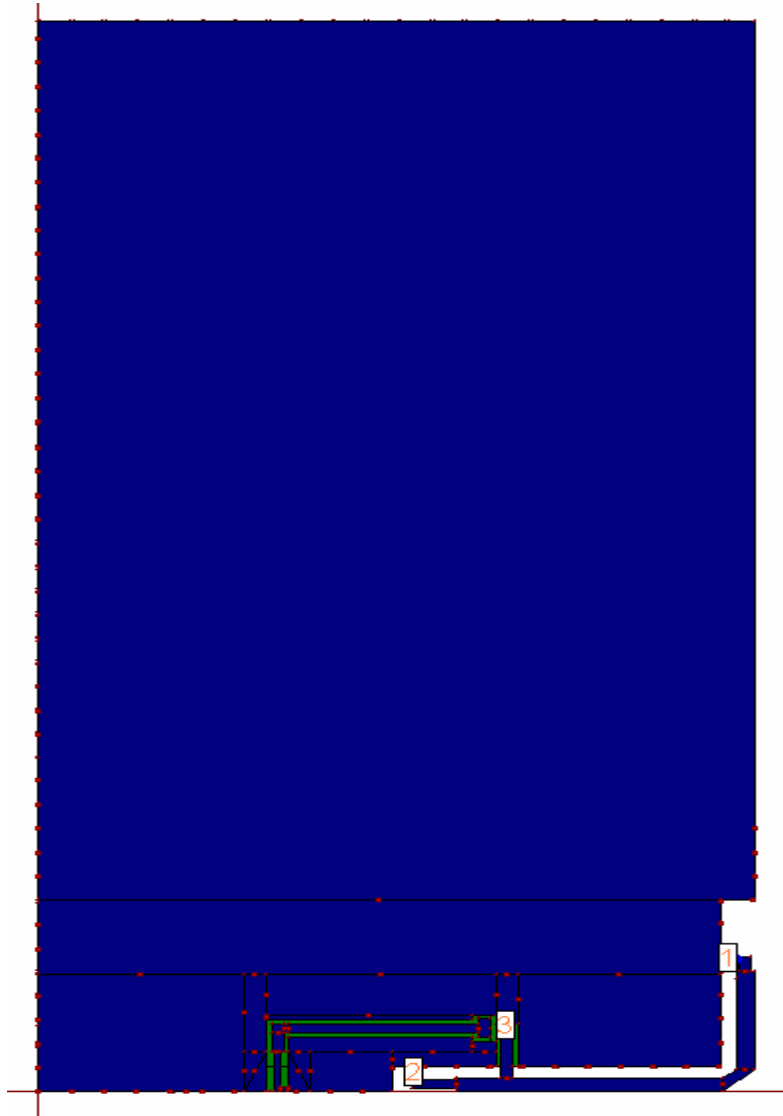


Figure 36: Structure of the simulated antenna

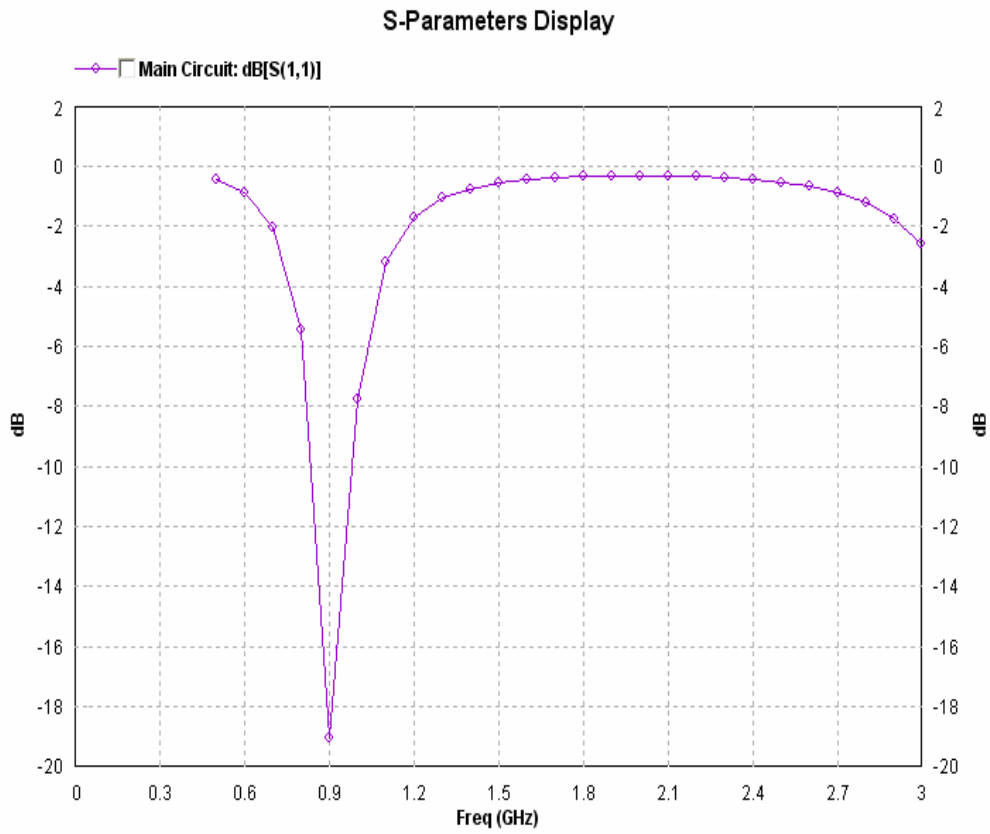


Figure 37: Return loss of the onboard PCB antenna from simulation

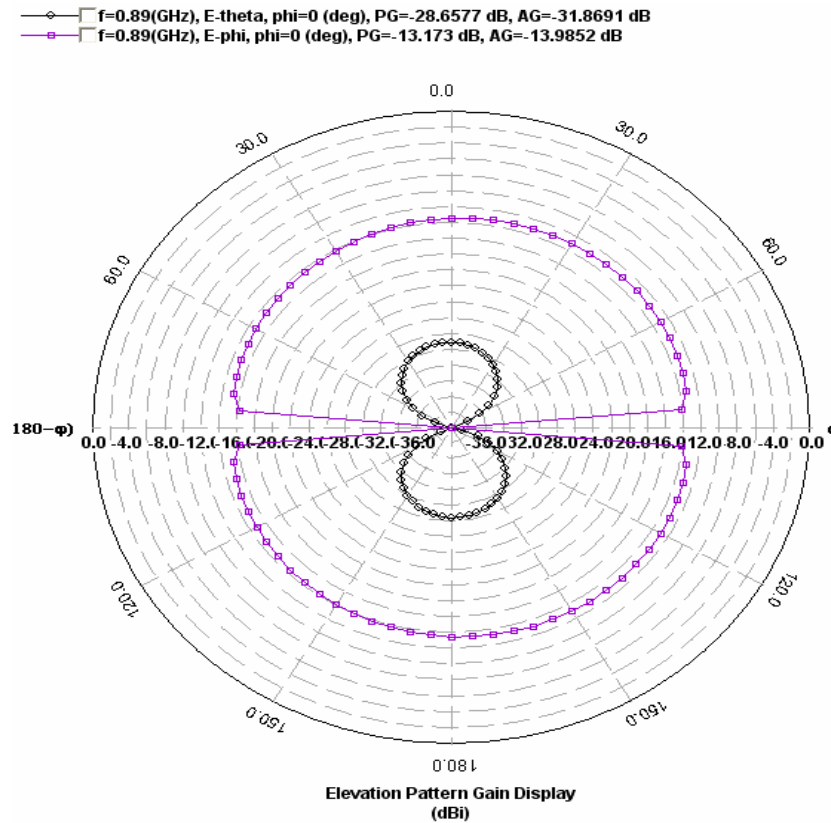


Figure 38: Simulated pattern of the on-board PCB antenna

3.4 Suitable Candidate Antennas for Short-Range Radio Applications

Printed Dipole

The radiation pattern of the printed dipole is very close to the pattern of an ideal dipole. But it is relatively large in structure and requires differential feed that makes it unsuitable for small portable devices.

Microstrip Patch

We can get both linear and vertical polarization for the microstrip patch antenna. The production cost of such antennas is also low. But, the bandwidth of such antenna is very narrow that makes it unsuitable for many applications.

Ceramic Antenna

As wireless equipment size shrinks and functional demands grow, miniaturized ceramic chip antennas are available in the market. For such types of antennas, the antenna characteristics highly depend on the dielectric constant of the ceramic materials and the silver layer. Various laminating techniques are used for the accuracy requirements and to improve antenna performance. The extended bandwidth is one of the advantages of this kind of antenna. But the antenna does not have negligible cost per unit.

Monopole and its variants

The inverted-L and the inverted-F antennas fall under this category. The inverted-F antenna is well known for its ability to provide flexibility in impedance matching, and to produce vertically and horizontally polarized electric fields[14], a feature desirable for indoor environments.

4 CONCLUSION

A wireless device needs to be tested comprehensively before being put in an application. Communication range is an extremely important factor in characterizing a wireless device. This work characterized a wireless transceiver, with special emphasis on TRF6901, with respect to the TRF6901/MSP430 demonstration and development board. The board with RF section as TRF6901 and its matching components driven by a baseband processor MSP430, employs an inverted-F antenna (IFA). Since the antenna characteristics were not provided by the supplier, a detailed design analysis of the employed antenna was done by simulating in IE3D, a commercial method of moment software packages from Zeland [13]. The simulation results were verified by taking experimental measurements in the laboratory environment, a semi-anechoic chamber. It is seen that the employed antenna has the ability to receive both horizontally and vertically polarized electromagnetic waves. For indoor environments where the depolarization phenomenon makes the choice of polarization difficult, this type of antenna can be the best possible choice. The range of the board was also measured with an external sleek dipole antenna with a relatively higher gain than the on-board pcb antenna. It shows that there is a slight benefit of the external dipoles over the IFAs.

Although, many wireless devices use the vertically polarized antennas, it was found that using horizontal polarization both at the receiver and at the transmitter results in 10 dB more power in the median than using vertical polarization both at the receiver and the transmitter [15].

LIST OF REFERENCES

1. B. Alan, Short-range Wireless Communication, LLH Technology Publishing, 2000.
2. Proakis, John, Digital Communications, McGraw-Hill College, 2000.
3. TRF6901 Single-Chip RF Transceiver, TI data sheet SLWS 110E, September 2001.
4. TRF6901 Design Guide, TI application report SWR035, April 2002.
5. Fractional/Integer-N PLL Basics, TI technical brief SWRA029.
6. Rappaport, Theodore S., Wireless Communications Principles and Practice, Prentice-Hall, 1996.
7. B. Sklar, Digital Communications Fundamentals and Applications, Prentice-Hall, Inc. 1988.
8. Designing with the TRF6900 Single-Chip RF Transceiver, TI application report SWRA033D, June 2001.
9. Ziemer, R.E., Tranter, W.H., Principles of Communication Systems, Modulation and Noise, 4th Edition, John Wiley and Sons, 1995.
10. TRF6901 Demonstration and Development Kit, User's Guide, TI publication, August 2003.
11. MSP430F449 data sheet, TI publication, August 2004.
12. C.A Balanis, Antenna Theory, Analysis and Design, Second Edition, New York, Wiley and Sons Inc., 1998.
13. IE3D User's Manual, Zealand Software Inc., Version 10.1

14. Z. N. Chen, K. Hirasawa, K. W. Leung, and K. M. Luk, "A New Inverted F Antenna with a Ring Dielectric Resonator," IEEE Transactions on Vehicular Technology, VT-48, July 1999, pp. 1029-1032.
15. D. Chizhik, J. Ling, and R. A. Valenzuela, "The Effect of Electric Field Polarization on Indoor Propagation," IEEE ICUPC, Florence Italy, 1998.